Molecular Biology of the Cell
Vol. 21, 117–130, January 1, 2010

A Novel c-Jun N-terminal Kinase (JNK)-binding Protein WDR62 Is Recruited to Stress Granules and Mediates a Nonclassical JNK Activation

Tanya Wasserman,*† Ksenya Katsenelson,*† Sharon Daniliuc,*† Tal Hasin,* Mordechay Choder,‡ and Ami Aronheim*

Departments of *Molecular Genetics and ‡Microbiology, The Rappaport Family Institute for Research in the Medical Sciences, Technion-Israel Institute of Technology, Haifa 31096, Israel

Submitted June 22, 2009; Revised October 27, 2009; Accepted October 29, 2009
Monitoring Editor: Jonathan Chernoff

The c-Jun N-terminal kinase (JNK) is part of a mitogen-activated protein kinase (MAPK) signaling cascade. Scaffold proteins simultaneously associate with various components of the MAPK signaling pathway and play a role in signal transmission and regulation. Here we describe the identification of a novel scaffold JNK-binding protein, WDR62, with no sequence homology to any of the known scaffold proteins. WDR62 is a ubiquitously expressed heat-sensitive 175-kDa protein that specifically associates with JNK but not with ERK and p38. Association between WDR62 and JNKs occurs in the absence and after either transient or persistent stimuli. WDR62 potentiates JNK kinase activity; however it inhibits AP-1 transcription through recruitment of JNK to a nonnuclear compartment. HEK-293T cells transfected with WDR62 display cytoplasmic granular localization. Overexpression of stress granule (SG) resident proteins results in the recruitment of endogenous WDR62 and activated JNK to SG. In addition, cell treatment with arsenite results in recruitment of WDR62 to SG and activated JNK to processing bodies (PB). JNK inhibition results in reduced number and size of SG and reduced size of PB. Collectively, we propose that JNK and WDR62 may regulate the dynamic interplay between polysomes SG and PB, thereby mediating mRNA fate after stress.

INTRODUCTION

Mitogen-activated protein kinases (MAPKs) regulate a variety of cellular processes in response to extracellular signals. MAPKs are activated through a protein kinase cascade in which a MAP 3K activates a MAP 2K that in turn activates a MAPK (Shaul and Seger, 2007). Three main modules exist in mammals: the extracellular regulated kinases (ERK), stress-activated protein kinases (SAPK, also known as c-Jun N-terminal kinase, JNK) and p38. In many instances, these MAPK modules have been shown to regulate distinctly different cellular responses in a cell type– or signal-specific manner. During the last decade, the importance of scaffold proteins was described as providing signal specificity and fidelity (Weston *et al.*, 2002). Scaffold proteins act as multidomain interacting surfaces that serve as a meeting platform for kinases and substrates to orchestrate specific transmission of signaling. By the interaction with two or more components of the cascade, scaffold proteins increase the efficiency of signaling by concentrating proteins locally and positioning kinases in close proximity to their substrates. The association of the signaling components with the scaffold protein allows signal channeling to a specific outcome. In addition, some of the scaffold proteins are able to allosterically activate the associated kinase or, alternatively, they may restrict the activation of the signaling pathway to a specific subcellular compartment (Dard and Peter, 2006). Multiple scaffold proteins were described for the MAPK cascade and found to enhance signal transduction by promoting the assembly of multiprotein complexes (Tibbles and Woodgett, 1999; Davis, 2000; Chang and Karin, 2001; Rubinfeld and Seger, 2005).

Several scaffold proteins were described for the JNK signaling pathway; for example, β-arrestin is a scaffold protein shared by the ERK cascade as well as the SAPK cascade. β-arrestin specifically links the activation of seven transmembrane receptor to JNK3 activation (Miller and Lefkowitz, 2001); CrkII mediates the activation of Rac1 in cells exposed to EGF (Girardin and Yaniv, 2001); Filamin mediates the activation of JNK by TNF-α receptor signaling (Marti *et al.*, 1997); and the JNK-interacting proteins (JIP 1-3), which are able to associate with all the components of the SAPK module and additional signaling proteins and potentiate JNK activity. The JIPs can associate with both positive and negative regulators of JNK (Morrison and Davis, 2003). In addition, all three JIPs are able to associate with the tetracopeptide repeat domain of the light chain of the microtubule motor protein kinesin-1 and thus can be transported as cargo molecules along the microtubule network within cells (Verhey *et al.*, 2001). Numerous JNK-associating proteins were also described to regulate JNK activity such as JAMP, a seven-transmembrane protein that binds JNK and

This article was published online ahead of print in *MBC in Press* (http://www.molbiolcell.org/cgi/doi/10.1091/mbc.E09–06–0512) on November 12, 2009.

† These authors contributed equally to this work.

Address correspondence to: Ami Aronheim (aronheim@tx.technion.ac.il).

Abbreviations used: JBP, JNK-binding protein; JNK, c-Jun N-terminal kinase; HEK-293, human embryonic kidney 293; MAPK, mitogen-activated protein kinase; PB, processing bodies; SG, stress granules; WDR62, WD repeat domain 62.

is responsible for the increase in the duration of JNK signaling after stress (Kadoya *et al.*, 2005) and JNKBP1, which enhances JNK activation by MEKK and TGFβ-activated kinase 1 (TAK1; Koyano *et al.*, 1999). In addition, we have previously identified IKAP as a scaffold protein for the JNK pathway displaying functional interaction with JNK, MAP3K, and ASK1 (Holmberg *et al.*, 2002).

In an attempt to isolate novel JNK-binding proteins, we have used a kinase inactive JNK1 as bait to screen a cDNA expression library using the yeast Ras recruitment system, RRS, (Broder *et al.*, 1998). WDR62 was identified after this screen encoding a cDNA of a previously uncharacterized protein with little sequence homology with known proteins. The current manuscript describes for the first time the characterization of WDR62 and its possible role in mediating mRNA homeostasis after stress.

MATERIALS AND METHODS

Antibodies and Reagents

Arsenite (Fluka, Ronkonkoma, NY; 71287) was dissolved in PBS to generate 50 mM stock solution. Puromycin (Sigma-Aldrich, St. Louis, MO; P7255) was dissolved in DDW to generate 2 mg/ml stock solution. SP600125 (Calbiochem, La Jolla, CA; 420119) was dissolved in DMSO to generate 20 mM stock solution. Collagen (Roche, Indianapolis, IN; 11179179001) was dissolved in 0.2% acetic acid to generate 2 mg/ml stock solution.

The following antibodies were used: anti-Myc monoclonal (9E10), anti-HA monoclonal (12CA5), anti-Flag (M2) monoclonal (Sigma-Aldrich), anti-α-tubulin monoclonal (Sigma-Aldrich), anti-c-Jun polyclonal (Santa Cruz Biotechnology, Santa Cruz, CA), anti-phospho-c-Jun polyclonal (Cell Signaling, Beverly, MA), anti-phospho-JNK polyclonal (Sigma-Aldrich), anti-TIA1 polyclonal (Santa Cruz), anti-DCP1α monoclonal (Abnova), anti-G3BP monoclonal (BD Laboratories, Lexington, KY), and anti-JIP polyclonal (Santa Cruz).

The antibodies anti-JBP5 polyclonal, anti-JBP774 polyclonal, and anti-WD40 polyclonal were prepared by rabbit immunization with the appropriate GST tagged peptide (the amino acids position corresponding to the peptide fragments used are depicted in Figure 1A). Anti-JBP5 antibody was affinity-purified. Initially, serum was precleared on a GST-attached Sepharose beads followed by absorption on GST-JBP5 attached Sepharose beads. IgG was eluted by 0.2 M glycine, pH 2.5, titrated directly into 2 M Tris-HCl buffer, and dialyzed against PBS containing 10% glycerol. Anti-WD40 clone 3G8 monoclonal was generated against GST-WD40 purified protein (Sigma-Aldrich).

Fluorochrome-tagged secondary antibodies for immunofluorescence assays were obtained from Jackson ImmunoResearch Laboratories (West Grove, PA).

Plasmids

The mammalian expression plasmid pCAN was used to express Myc-WDR62 and Myc-JBP5. GST-WD40 (aa 1-208), GST-JBP5 (aa 1018-end), GST JBP774 (aa 969-1109), GST-JBP5Δ7SP (aa 1018-1265), and GST-JBPΔ6SP (aa 1018-1326) were expressed using the pGEX kg bacteria expression plasmid.

Yeast plasmids used: pMyr-JBP5 and pMyr-WDR62-C encoding WDR62 starting from aa 1018 and 1215, respectively, fused to v-Src myristoylation signal in the pMyr yeast expression plasmid (Stratagene, La Jolla, CA). pMet425-JNK1KM-Ras encodes a kinase inactive JNK1 mutant (K149M). JNK1KM is unable to bind ATP as described in Holmberg *et al.* (2002). All other yeast expression plasmids were previously described (Hubsman and Aronheim, 2001).

The following plasmids used, HA-MKK7, HA-JNK1, and HA-JNK2, were expressed using the SRα mammalian expression plasmid (Xia *et al.*, 1998). HA-JNKK2-JNK1 was previously described (Zheng *et al.*, 1999).

Fluorescent-tagged expression plasmids were kindly provided as follows: YFP-TIA1 and YFP-TTP by Dr. N. Kedersha (Harvard Medical School, Boston, MA), GFP-G3BP by Dr. J. Tazi (Institut de Génétique Moléculaire de Montpellier, Montpellier, France), M1-CFP by Dr. M. Philips (New York University School of Medicine, New York, NY), and GFP-JNKs (1-3) by Dr. M. Courtney (University of Kuopio, Kuopio, Finland).

Cell Culture and Transient Transfection

Human embryonic kidney 293T (HEK-293T), HEK 293, HeLa, MEF, and H1299 were maintained in DMEM containing 10% FCS and 1% penicillin and streptomycin and grown at 37°C and 5% CO_2. HEK-293T cells were transfected with the appropriate expression plasmid using the calcium-phosphate (Ca_2PO_4) method. The total amount of plasmid DNA was adjusted to 10-12 μg in a total volume of 1000 μl. Cells were replaced with fresh medium 4-5 h after transfection and harvested 24 h after transfection.

Assays

For the luciferase reporter assay, cells were grown in 60-mm dishes, and transfection was performed in a total volume of 500 μl. For the immunofluorescence assay, cells were grown in six-well plates, and transfection was performed in a total volume of 400 μl. For the reporter assay, HEK-293T cells were cotransfected with expression plasmids and reporter plasmid 4 X AP1-luc. Luciferase activity was assayed using the Luciferase Assay System (Promega, Madison, WI) as described in the manufacturer's protocol.

Ras Recruitment System

Yeast growth, transfection, and screening protocol were performed as described in Hubsman and Aronheim (2001).

Western Blot

Cells were lysed in whole cell extract (WCE) buffer (25 mM HEPES, pH 7.7, 0.3 M NaCl, 1.5 mM $MgCl_2$, 0.2 mM EDTA, 0.1% Triton X-100, 0.5 mM DTT, 20 mM β-glycerolphosphate, 0.1 mM Na_2VO_4, 100 μg/ml PMSF, Protease inhibitor cocktail 1:100; Sigma-Aldrich, P8340). The proteins were then separated by 10% SDS-PAGE, followed by a transfer to nitrocellulose membrane. Blots were blocked in 5% dry milk in PBS and washed three times for 5 min in PBS. All primary antibodies were diluted 1:500 except for the following: anti-α-tubulin 1:2000, anti-Flag 1:1000, and anti-JIP 1:100. Primary antibodies were incubated for at least 1 h at 4°C. Primary antibodies were detected using the corresponding HRP-conjugated secondary antibodies obtained from Sigma-Aldrich.

Coimmunoprecipitation

Antibodies against hemagglutinin (HA), Myc, or Flag were incubated overnight at 4°C with 400-600 μg of the HEK-293T protein extract. Protein A Sepharose beads (Sigma-Aldrich) were added to the extracts for 1 h at 4°C. After four washes with WCE buffer, the precipitated proteins were eluted using SDS-PAGE sample buffer. Samples were boiled for 3 min and then processed for Western blot analysis.

Kinase Assay

HEK-293T cells were cotransfected with the indicated amounts of WDR62 encoding plasmid together with 3 μg of either HA-JNK1 or 2, HA-ERK1, or HA-p38α. The total DNA content was kept constant by adding the corresponding empty expression vector. Twenty-four hours after transfection, cell lysate was prepared and rotated for 1 h at 4°C with protein A beads (Santa Cruz) that were preincubated with anti-HA antibodies. In vitro kinase assay was performed using purified glutathione *S*-transferase (GST) c-Jun_{1-79} as JNK substrate or myelin basic protein and His-JDP2 as ERK and p38 substrates, respectively. The reaction was performed in the presence of [γ^{32}P]ATP for 30 min at 30°C. Reactions were stopped by the addition of SDS-PAGE sample buffer. The samples were then boiled, and the phosphorylated proteins were resolved by 10% SDS-PAGE. The gel was dried and subjected to radiography. Phosphorylated c-Jun_{1-79} product incorporating ^{32}P was quantified by PhosphoImager analysis (FLA 2000, Fujifilm, Stamford, CT). Fold activation of JNK1 and JNK2 was determined using TotalLab software (Newcastle upon Tyne, United Kingdom), taking into consideration the variations of expressed proteins.

RT-PCR

Semiquantitative RT-PCR was performed using Verso cDNA kit (Thermo Fisher Scientific, Rochester, NY) according to the manufacturer's instructions. mRNA was prepared by Trizol reagent (Sigma-Aldrich) according to the manufacturer's instructions.

The following primers were used: WDR62 CS1 F: GAAGTGGAAATCTGAGGCAAG; WDR62 CS1 R: GAAGTGCAGCTCGTGGATC; WDR62 CS2 F: CGCCACCACTTTGAGACAC; WDR62 CS2 R: TTCAGCTTCAGAGGCCTCCA; WDR62 CS4 F: GGACAGCAGCCCTGATTCTC; WDR62 CS4 R: GCAGAGCAGGAGCCAAATTG; WDR62 CS5 F: CTCTTCCCCGCAGCTCTG; and WDR62 CS5 R: ATGGGTGAACCTGGATGCC.

For WDR62 mRNA expression in human tissues the following were used: human WDR62-F (2372) 5′-CCGGAATTCTCCCTGAGCCCTGGAGAG; and human WDR62-R (2738) 5′-CCGCTCGAGACTCACTCAGCAGGCTGGC. For WDR62 mRNA levels following stress the following were used: human WDR62-F (1564) 5′-CCGGAATTCATCTCCCTCGGTGACAGTGAG; human WDR62-R (Δ6SP) 5′-CCCGCTCGAGTCAGCGAAAGGCAGAGCCGTG; human GAPDH-F 5′-CATCACCATCTTCCAGGAGCGA; and human GAPDH-R 5′-GTCTTCTGGGTGGCAGTGATGG.

Cellular Treatments

HEK-293T cells were treated with 0.5 mM arsenite for the indicated time or with 20 μM SP600125 for 1 h before arsenite treatment. UV-C irradiation was performed using an 8 W bulb at 30 cm distance for 1 min. The medium was removed before irradiation. The medium was reintroduced, and cells were returned to the incubator for 30 min before harvesting.

Stress Granule and Processing Body Induction for Immunofluorescence

HEK-293T cells were treated for 1 h with either 20 mg/ml puromycin or 0.5 mM arsenite or treated for 2 h with 0.5 mM arsenite with the addition of 20 mg/ml puromycin after 1 h of arsenite treatment. Heat shock was performed by incubating HEK-293T cells at 44°C for 30 min.

Immunofluorescence

HEK-293T cells were grown on glass cover-slips coated with collagen. After transfection or cellular stimulation, cells were fixed with 4% formaldehyde for 10 min. After washing with PBS, the cells were permeabilized with 0.1% Triton X-100 for 5 min and incubated in a blocking solution of 5% FCS in PBS for 30 min. The cells were then incubated with the appropriate primary antibody mixture for 1 h in PBS containing 1% FCS. The cells were washed three times with PBS and incubated with a secondary fluorescent antibodies mix for 1 h in PBS containing 2% BSA, 2% FCS, and 0.1% Tween-20. The cells were washed twice with PBS and processed for nuclear staining using DAPI (Sigma-Aldrich, D9542) at a final concentration of 1 $\mu g/\mu l$ in PBS. The stained cells were then washed twice with PBS and mounted in Fluoromount-G (Southern Biotechnology, Birmingham, AL, 0100-01).

Confocal Microscopy

Fluorescence microscopy was performed using the Zeiss LSM 510 Meta inverted confocal microscope (Thornwood, NY) equipped with a 63×/1.4 NA oil objective, multiline Ar laser (488, 514 nm), DPSS laser (561 nm), HeNe laser (633 nm), and a UV Diode laser (405 nm). Each image was acquired from a single 1-μm thickness Z-stack using 510 LSM software (Zeiss).

Quantifications and Colocalization Analysis and Statistical Analysis

Image acquisition was performed with six Z-stacks with 0.5-μm intervals using the 510 LSM software (Zeiss). Colocalization analysis was performed on the midplane of each image. Weighted colocalization coefficient was calculated by the software for each channel. For quantification analysis, projection was applied on each image. The size and the number of stress granules (SGs) and processing bodies (PBs) were calculated using the ImageJ software (http://rsb.info.nih.gov/ij/). Statistical analysis was performed using Student's unpaired *t* test with one-tailed distribution.

RESULTS

Isolation of WDR62

To identify novel JNK-interacting proteins, the Ras recruitment system was used to screen human cDNA expression libraries derived from either skeletal muscles or testes. The bait used encoding a catalytically inactive JNK1 protein (JNK1KM) fused in frame with the cDNA encoding the cytoplasmic Ras protein (Holmberg *et al.*, 2002). The expression of the JNK1KM-Ras bait was designed under the control of the Met425 promoter, whereas the expression of the corresponding cDNA library is fused to the v-Src myristoylation signal under the control of the Gal1 promoter (Hubsman and Aronheim, 2001). A Cdc25-2 yeast strain was cotransfected with the bait and prey library expression plasmids and selected on glucose plates lacking uracil and leucine. Transformants were replica plated into galactose containing medium lacking methionine and grown at the restrictive temperature of 36°C. Yeast colonies growing under these conditions were selected and further analyzed. Plasmid DNA was isolated from the clones and reintroduced into the Cdc25-2 yeast strain with either the specific JNK1KM-Ras bait or nonspecific bait (Ras-Pak). Yeast transformants that exhibited specific growth with JNK1KM-Ras bait at the restrictive temperature but not with the nonspecific bait were subsequently subjected to DNA sequencing. One of the clones designated as a JNK-binding protein 5 (JBP5) displayed JNK1KM specific growth (Supplemental Figure S1A). JBP5 was isolated independently from both libraries and encodes the 505-amino acid C-terminal part of WDR62 (gene accession number NM_173636). A shorter WDR62 fragment encoding 309 aa from the C-terminus (WDR62-C) was still able to associate with JNK1KM bait (Supplemental Figure S1A). In contrast, yeast transformants with prey plasmid encoding Chp protein were able to grow at the restrictive temperature only with Ras-Pak bait but not with JNK1KM bait (Supplemental Figure S1A). WDR62 encodes 1523 amino acids of a previously uncharacterized protein that displays no sequence homology with a known gene in the databank. A schematic representation of WDR62 protein is shown in Figure 1A. The N-terminal domain of the protein encodes multiple WD40 repeats found in numerous regulatory proteins such as βTRCP and Cdc4 (Garcia-Higuera *et al.*, 1996).

WDR62 Expression Pattern in Tissues

To reveal WDR62 expression, we used a cDNA expression panel derived from mRNA prepared from 24 human tissues. A PCR reaction with WDR62 specific primers (Figure 1B, red arrows) resulted in an expected 366-base pair fragment in all tissues at a variable intensity with the highest expression in the heart, skeletal muscles, and testes (Supplemental Figure S1B). Based on the gene expression data (Ensembl database, ENSG00000075702), five potential alternative splice variants for WDR62 were suggested (Figure 1B). CS2 and CS5 represent the full-length cDNAs, which differ by 15 base pairs that are absent in CS2. Transcripts CS3 and CS4 correspond to N-terminal encoding WDR62 transcript except for the last 11 and 81 base pairs, respectively (Figure 1B, denoted as green line). CS1 transcript is identical to CS2/CS5 only for the first 129 base pairs but is differ along the entire transcript. To examine which of the transcripts is expressed in human cell lines, oligonucleotides were designed to selectively recognize the full-length and truncated transcripts (Figure 1B, blue arrows). To determine the specificity of the oligonucleotides designed, we first tested the cDNA corresponding to the CS5 transcript as a template for the PCR reaction with the designed oligonucleotides (Figure 1C). Indeed, only the oligonucleotides designed to recognize CS2 and CS5 transcripts were able to produce a specific band at the expected size that corresponded to the CS5 transcript. Next, PCR analysis was performed with cDNA derived from human embryonic kidney cells (HEK-293T). This analysis revealed that CS5 represent the major full-length transcript in HEK-293T cells (Figure 1D, lanes 3 and 7), whereas within the truncated transcripts, the N-terminal CS4 transcript is present but not the C-terminal CS1. Similar results were obtained with other human cell lines such as HEK-293, HeLa cells, and H1299 lung carcinoma (Supplemental Figure S1C). This analysis was not definitive for the CS3 transcript, since no primers could be designed to specifically detect the CS3 transcript among the other putative N-terminal transcribed mRNAs (CS2, CS5, and CS4).

WDR62 Expression in HEK-293T Cells

We cloned the full-length cDNA of the major WDR62 (CS5 transcript) into a pcDNA-based mammalian expression plasmid fused to an N-terminal cMyc epitope-tag. In addition, we have generated three rabbit polyclonal antibodies and a mouse mAb as shown in Figure 1A. HEK-293T cells were transfected with the Myc-WDR62 expression vector followed by coimmunofluorescence analysis. Fixed cells were costained with anti-Myc (9E10) together with each one of the corresponding WDR62 rabbit polyclonal antibodies described above. We used the appropriate secondary antibodies to recognize the mouse and rabbit primary antibodies with Cy2 (green) and rhodamine (red) fluorescence, respectively. Both the monoclonal and the polyclonal antibodies reacted with the transfected WDR62 and exhibited a similar granular cytoplasmic staining (Figure 2A). In addition, we

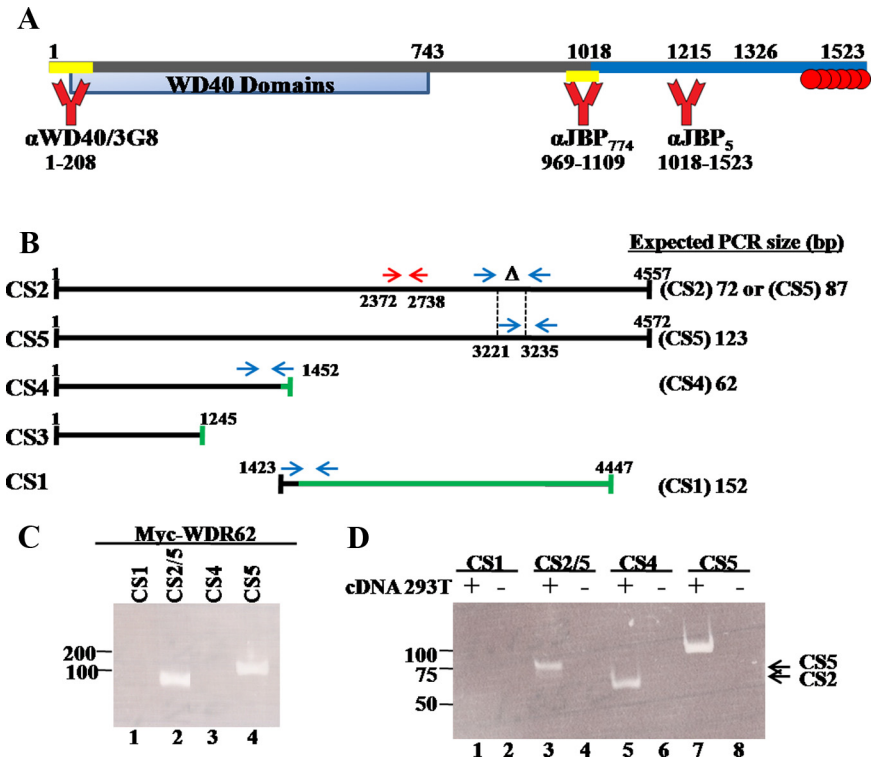

Figure 1. WDR62 cloning and expression pattern. (A) Schematic diagram of the WDR62 protein. Numbers represent the position of amino acids. JBP5 (blue bar) and WDR62-C fragments starts at position 1018 and 1215, respectively. The domain containing the 12 WD40 domains is depicted in light blue (WD40 domains). The domains against which antibodies were generated are indicated at the bottom (yellow bar). Six potential MAPK phosphorylation sites located at the C-terminal domain are indicated as red circles. (B) Schematic representation of the predicted five spliced variants. Black line represents region with sequence identity to the major full-length transcripts, CS2 and CS5. Green line corresponds to region with no sequence homology to CS2 and CS5 transcripts. Oligonucleotides (depicted as blue arrows) were designed to recognize specifically four splice variant transcripts except for the CS3 transcript. The expected size of the PCR fragment for each splice form is indicated on the right. Red arrows represent the oligonucleotides used to prepare the probe for the tissue cDNA array (Supplemental Figure S1B). (C) PCR was performed with plasmid containing CS5 cDNA or (D) cDNA prepared from HEK-293T cells with the indicated oligonucleotides. PCR was performed in the absence (−) or presence (+) of cDNA template. Samples were separated on a 15% nondenaturing PAGE. DNA size markers are indicated. The migration of CS5 and CS2 PCR products is indicated at the right.

stained HEK-293T cells transfected with the WDR62 encoding plasmid with the WDR62 mAb (3G8) followed by rhodamine fluorescence (red) secondary antibody to recognize the mouse primary antibody and obtained identical pattern of WDR62 expression (Figure 2A). Surprisingly, cell lysate derived from HEK-293T cells transfected with WDR62 encoding plasmid, and separated by SDS-PAGE followed by Western blot analysis failed to detect the transfected Myc-WDR62 protein (Figure 2B lane 6). Once boiling was avoided and the sample was either loaded without heating or heated for 5 min up to 50°C, a single cross-reacting protein at the expected 175-kDa size was observed (Figure 2B, lanes 2-4).

We next examined whether or not the endogenous WDR62 protein displays a similar heating sensitivity. Toward this end, cell lysate derived from HEK-293T cells was either not heated or preheated before gel loading as indicated and subjected to Western blot analysis with anti-JBP5 antibody (Figure 2C). Consistently, the endogenous WDR62 protein migrates to similar size and displays preheating sensitivity before SDS-PAGE loading (Figure 2C). Similarly, all three polyclonal antibodies generated against WDR62 recognize the transfected and the endogenous heat-sensitive WDR62 protein (Supplemental Figure S2A). The mAb 3G8 displays low sensitivity in Western blot analysis; however, it is highly specific for immunofluorescence (Figure 2A). We took advantage of the preheating sensitivity of WDR62 protein to identify the endogenous protein in different cell lines. Western blot analysis with different human cell lines revealed that WDR62 protein is expressed as a heat-sensitive protein in multiple human cell lines (Figure 2D). WDR62 protein sometimes appears as a doublet of 147 and 175 kDa. The origin of the different migration states may be due to different conformations that the protein acquires as a result of avoiding preheating of the sample before gel loading or represents a proteolytic product. Consistently, Western blot analysis with the three other anti-WDR62 antibodies resulted in similar results with variable background (Supplemental Figure S2B). Interestingly, a faint cross-reactive band was identified in mouse embryonic fibroblast cells (Figure 2D, lane 3, marked with an asterisk). The mouse WDR62 shares 75% amino acids identity with its human counterpart. HEK-293T cell lysate derived from cells transfected with a plasmid encoding the mouse WDR62 is recognized by anti-JBP5 antibodies alike the human counterpart (Supplemental Figure S2C).

WDR62 Interaction with the JNK Module

To confirm the interaction between WDR62 and JNK, we used immunofluorescence of HEK-293T cells cotransfected with different GFP-JNK isoforms, either alone or in the presence of WDR62 expression plasmid. The transfected WDR62 was detected with anti-3G8 monoclonal antibodies. Although GFP-JNKs (1-3) display mostly nuclear staining in the absence of WDR62, coexpression of GFP-JNKs with WDR62 protein results in colocalization of the GFP-JNKs and WDR62 in the previously shown cytoplasmic granules (Figure 3).

To examine the physical association between WDR62 and JNK, we used coimmunoprecipitation of cell lysate derived from transiently transfected HEK-293T cells. Expression plasmid encoding hemagglutinin (HA) epitope–tagged JNK2, was used in combination with an expression plasmid encoding the Myc epitope–tagged WDR62 fragment corresponding to JBP5 (C-terminal 505 amino acids). Western blot analysis

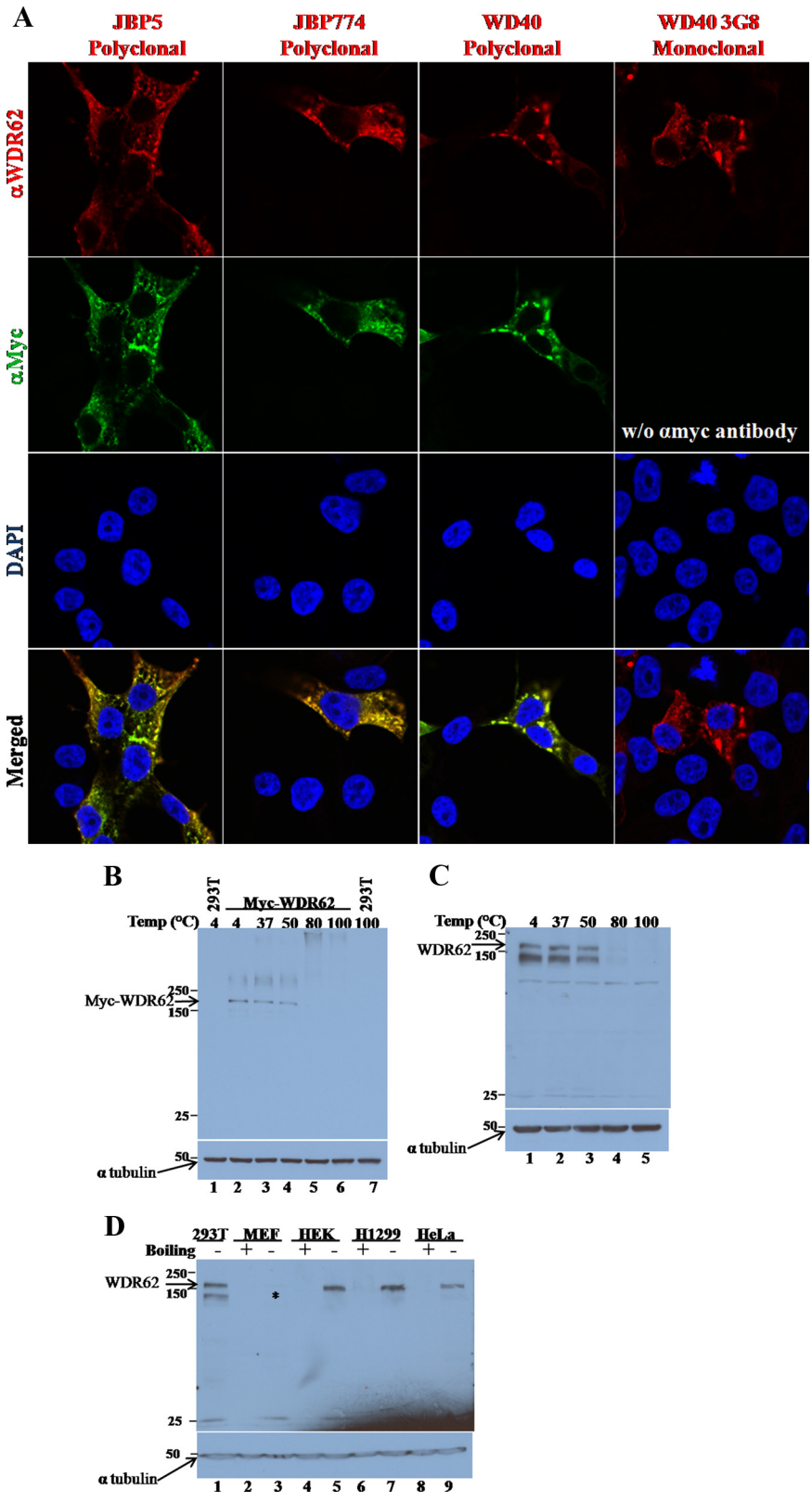

Figure 2. Transfected and endogenous WDR62 protein. (A) Immunofluorescence of fixed HEK-293T cells transfected with plasmid encoding Myc-WDR62. Cells were costained with affinity purified anti-JBP5, anti-JBP774, and anti-WD40 rabbit polyclonal antibodies (secondary antibody used rhodamine-conjugated donkey anti-rabbit, red) together with anti-Myc (9E10) mouse monoclonal antibodies (αMyc, secondary antibody used Cy2 conjugated donkey anti-mouse, green). Cells stained with mouse monoclonal anti-WDR62 (α3G8) (secondary antibody used rhodamine conjugated donkey anti-mouse, red). DAPI nuclear staining is shown (blue). Immunofluorescence was visualized by confocal microscopy. (B) Western blot analysis of HEK-293T cells either untransfected (−) or transfected (+) with pcDNA-based expression plasmid encoding Myc-WDR62. Cell lysate was prepared 24 h after transfection and separated by 8% SDS-PAGE. Samples were preheated before gel loading at the indicated temperature for 5 min. The expression level of WDR62 (anti-Myc, top panel) and α-tubulin (bottom panel) was examined with the corresponding antibodies. (C) Western blot analysis of HEK-293T cell lysate separated by 8% SDS-PAGE. Samples were preheated before gel loading at the indicated temperature for 5 min. The expression level of endogenous WDR62 (anti-JBP5, top panel) and α-tubulin (bottom panel) was examined with the corresponding antibodies. (D) Western blot analysis of lysate derived from different human cell lines including HeLa, H1299, HEK-293 (HEK), and HEK-293T (293T) or mouse embryo fibroblast (MEF). Samples were either boiled for 5 min before gel loading (+) or nonheated (−). Expression level of WDR62 (anti-JBP5, top panel) and α-tubulin (bottom panel) were examined with the indicated corresponding antibodies. WDR62 migration is indicated by an arrow and asterisk (*).

with total cell lysate derived from the transfected cells revealed high level of expression of the tagged-proteins encoded by the corresponding transfected plasmids (Figure 4A). Coimmunoprecipitation of cell lysate was performed with anti-HA mAb (12CA5) followed by extensive washes. Eluted proteins were resolved by SDS-PAGE, followed by Western blotting and probed sequentially with anti-HA and anti-Myc monoclonal antibodies. Control transfected cell ly-

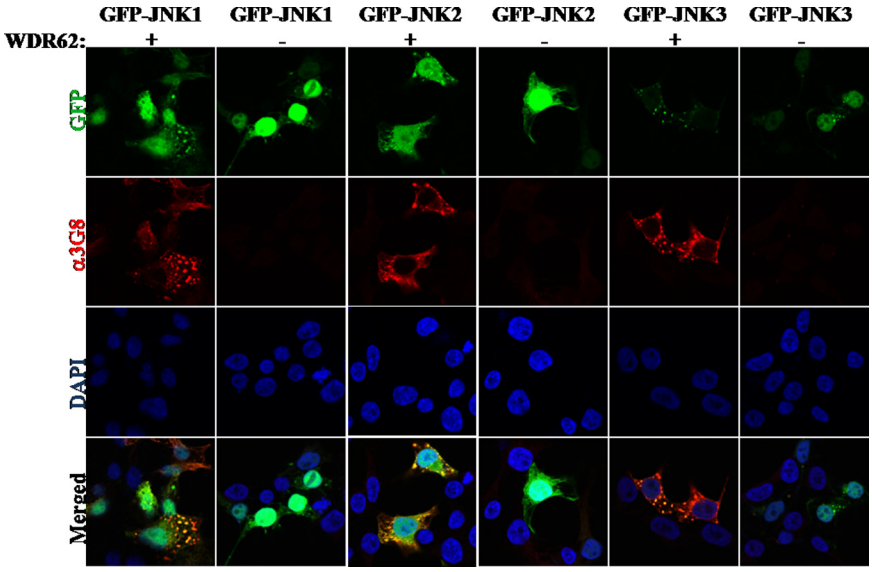

Figure 3. WDR62 associates with EGFP-JNKs in cells. HEK-293T cells were cotransfected with EGFP-JNKs together with either vehicle pCAN expression vector (−) or WDR62 (+). Cells were stained with anti-3G8 followed by the fluorescently labeled secondary antibody (α3G8, red fluorescence). Cells were visualized by confocal microscope.

sates lacking either Myc-JBP5 or HA-JNK2 failed to detect any cross-reactive protein with the anti-Myc antibodies (Figure 4A, left panel, lanes 5, 6, and 8). In contrast, Myc-JBP5 was efficiently precipitated by the anti-HA antibody only in the presence of HA-JNK2 (Figure 4A, left panel, lane 7). Conversely, coimmunoprecipitation with anti-Myc antibody was able to detect HA-JNK2 only in cell lysate derived from cells transfected with plasmids encoding both HA-JNK2 and Myc-JBP5 (Figure 4A, right panel, lane 3).

To examine whether or not WDR62 interaction with JNKs is specific to the stress-activated MAPK module, we examined the association of Myc-JBP5 with two other HA-tagged MAPK proteins ERK and p38 by coimmunoprecipitation. Transfected cell lysate were precipitated with anti-HA, subjected to SDS-PAGE and Western blotting, and probed sequentially with anti-HA and anti-Myc antibodies. Although Myc-JBP5 was efficiently precipitated with anti-HA antibody in the presence of HA-JNK1 (Figure 4B, lane 5), no precipitation was detected in precipitated lysate controls (Figure 4B, lanes 1–4) or in the presence of either HA-ERK1 or HA-p38α (Figure 4B, lanes 6 and 7). Western blot analysis with anti-HA antibody of total cell lysate and the immunoprecipitated anti-HA proteins demonstrated the presence of all the HA-tagged MAPK proteins at similar levels in the total cell lysate and anti-HA immunoprecipitation as well. Thus, we conclude that the interaction between the WDR62 fragment with JNK1 and JNK2 is specific to the JNK/SAPK signaling pathway.

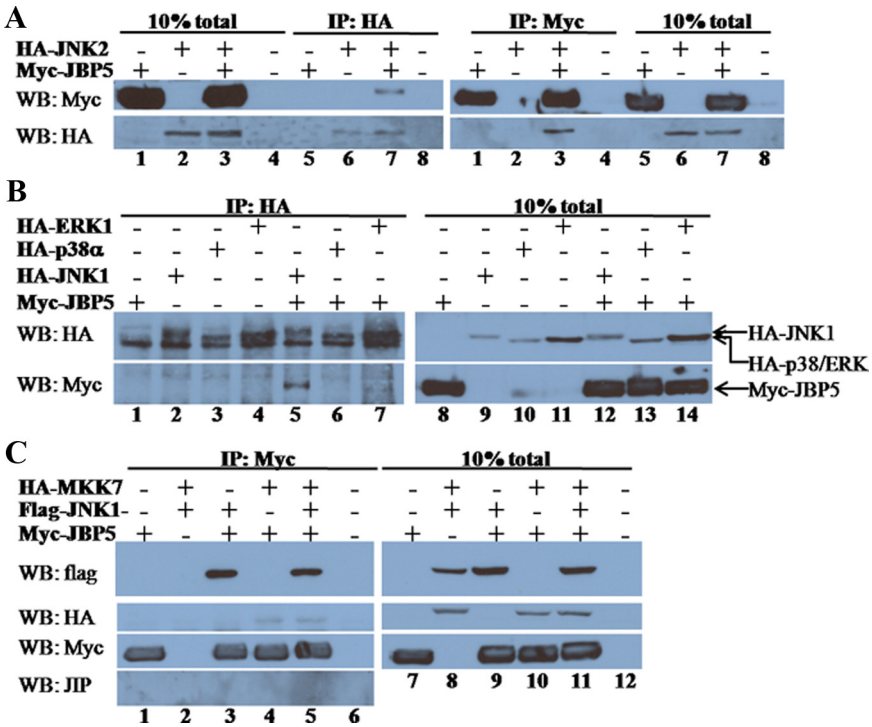

Figure 4. WDR62 associates with proteins from the JNK/SAPK tier. (A) HEK-293T cells were cotransfected as indicated. Cell lysate was coimmunoprecipitated with either anti-HA (left panel) or anti-Myc (right panel) and eluted proteins were separated by 10% SDS-PAGE, followed by Western blotting and probed with anti-Myc (top panel) and anti-HA (bottom panel) antibodies. Total cell lysate of transfected HEK-293T is shown (lanes 1–4 and 5–8, left and right, respectively). (B) HEK-293T cells were cotransfected as indicated. Cell lysate was coimmunoprecipitated with anti-HA antibody and eluted proteins (left panel) as well as total cell lysate (right panel) were separated by SDS-PAGE and Western blotting and probed with anti-HA (top panel) and anti-Myc (bottom panel) antibodies. The migration of the different transfected proteins is indicated (right panel). (C) HEK-293T cells were cotransfected as indicated. Cell lysate was coimmunoprecipitated with anti-Myc antibody and eluted proteins (left panel) as well as total cell lysate (right panel) were separated by SDS-PAGE, followed by Western blotting and probed with anti-Flag (top panel) and anti-HA (second top panel), anti-Myc (second bottom panel), and anti-JIP (bottom panel) antibodies.

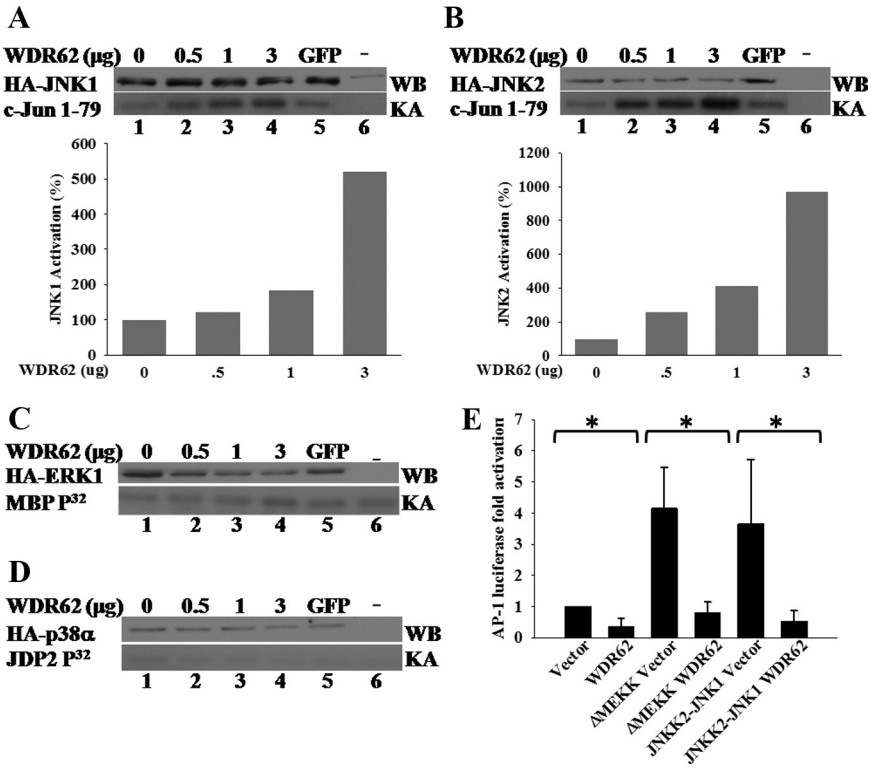

Figure 5. WDR62 potentiates JNK kinase activity, yet, results in reduced AP-1–dependent transcription. (A) In vitro kinase assay with HA-immunoprecipitated cell lysate derived from HEK-293 cells cotransfected with either HA-JNK1 (A) or HA-JNK2 (B) together with increasing amounts of Myc-WDR62 expression plasmid. The total amount of transfected plasmid DNA was adjusted with empty vehicle. The JNK kinase activity and expression levels in the presence of GFP encoding plasmid (3 μg) or untransfected cells are shown (A and B lanes 5 and 6, respectively). In vitro kinase assay was performed in the presence of [γ^{32}P]ATP and GST-c-Jun (5 μg) as substrate (bottom panel). Western blot analysis of transfected cell lysate was performed to assess the HA-JNK1 and HA-JNK2 expression level in each transfection (top panel). The extent of JNK activation relative to the activity obtained in the absence of WDR62 (100%) is shown (bottom). The results represent the mean of three independent experiments. (C and D) In vitro kinase assay with HA-ERK1 (C) and HA-p38 (D) was performed as described above except that MBP and GST-JDP2 was used as kinase substrates, respectively. Representative gel of two independent experiments is shown. (E) AP-1 luciferase reporter assay in HEK-293T cells. Cells were cotransfected with AP-1-luciferase reporter plasmid together with either vehicle (vector) or expression plasmids encoding either HA-ΔMEKK or HA-JNKK2-JNK1 in the presence or absence of Myc-WDR62 (WDR62). Twenty four hours after transfection luciferase activity was determined. The luciferase activity obtained from WDR62-transfected cells was normalized by setting the activity from vehicle-transfected cells as 1. The results represent the mean and SD of three independent experiments. * $p < 0.05$.

We next sought to test whether or not WDR62 is able to associate with the JNKs upstream MAP2K, MKK7. Toward this end, we used HEK-293T cells transfected with HA-MKK7, Flag-JNK1, and Myc-JBP5 in different combinations. Coimmunoprecipitation was performed with anti-Myc antibody, and subsequently Western blot was performed sequentially with anti-Flag, anti-HA, and anti-Myc (Figure 4C). This analysis revealed that anti-Myc antibody failed to precipitate the transfected Flag-JNK1 and HA-MKK7 from control lysate lacking Myc-JBP5 (Figure 4C, left panel, lane 2). In contrast, both Flag-JNK1 and HA-MKK7 were efficiently precipitated in the presence of Myc-JBP5 (Figure 4C, left panel, lanes 3-5). Interestingly, precipitation of HA-MKK7 occurred even in the absence of Flag-JNK1, suggesting that Myc-JBP5 is able to associate with HA-MKK7 as well (Figure 4C, left panel, lane 4). Similar results were obtained when anti-HA antibody was used in coimmunoprecipitation of cell lysates derived from HA-JNK2, HA-MKK7, and Myc-JBP5 in different combinations (Supplemental Figure S3A). The interaction of JBP5 with JNK and MKK7 could be either direct or mediated through a third protein. To examine the possibility that the JNK-interacting protein, JIP, is mediating WDR62 interaction with HA-MKK7 and/or Flag-JNK, we first examined the expression of JIP in HEK-293T cell lysate. Although JIP protein could be readily observed in lysate derived from rat hippocampus, we could not detect JIP expression in HEK-293T cells (Supplemental Figure S3B). These results are in accordance with previous reports showing the JIP 1-3 proteins are expressed at low levels in nonneuronal tissues (Yasuda *et al.*, 1999; Kelkar *et al.*, 2000). Consistently, no JIP protein was detected after coimmunoprecipitation with anti-Myc antibody of cell lysate derived from cells expressing the tagged JNK tier proteins (Figure 4C). Collectively, although we cannot rule out the possibility that MKK7-WDR62 interaction is mediated through binding to endogenous JNK protein, it seems likely that WDR62 is able to associate with the upstream MAP2K component of the JNK tier, MKK7. Thus, the ability of JBP5 to form a protein complex with both JNK1/2 and the upstream activator MKK7 suggests that WDR62 may act as a scaffold protein for the JNK module.

WDR62 Potentiates JNK Activity

The fact that WDR62 may play a role as a scaffold protein for the JNK tier prompted us to examine the ability of WDR62 to potentiate JNK kinase activity in the absence of a signal. Myc-WDR62 was cotransfected into HEK-293T cells at increasing amounts together with constant levels of either HA-JNK1 or HA-JNK2. Cotransfection of either vehicle control or GFP was used as control for the basal JNK activity. The HA-JNKs were precipitated with anti-HA antibodies, and the kinase activity was determined using bacterially purified GST-cJun (1-79) using in vitro kinase assay (Katz *et al.*, 2001). Both HA-JNK1 and HA-JNK2 kinase activity measured in the presence of Myc-WDR62 was augmented with the increasing amounts of WDR62 used in the transfection (Figure 5, A and B). No change in JNK kinase activity was observed with the GFP control lysate.

To examine the ability of WDR62 to potentiate the kinase activity of other MAPKs, we compared the kinase activity of either ERK1 or p38α in the absence or presence of increasing

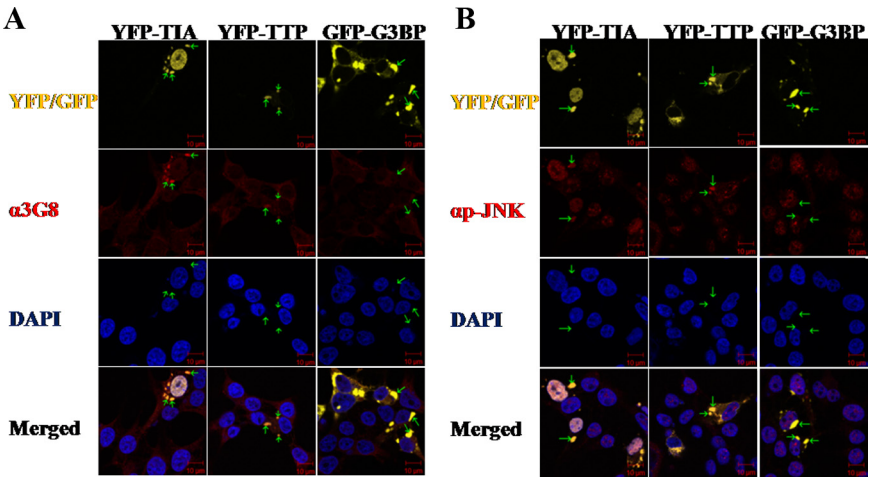

Figure 6. WDR62 and activated form of JNK are recruited to stress granules by YFP-TIA and YFP-TTP but not with GFP-G3BP. Immunofluorescence of HEK-293T cells transfected with the indicated fluorescently labeled proteins (shown all in yellow for simplicity). Fixed cells were immunostained with (A) anti-3G8 antibodies (α3G8, red) and DAPI nuclear stain (blue). (B) Anti-phospho-JNK (αp-JNK, red) and DAPI nuclear stain (blue). Representative images from confocal microscope are shown. Green arrows tag specific SG in each row to locate their position with the red filter.

expression of WDR62. In contrast to JNK, the kinase activity of neither ERK1 nor p38α kinase was affected in the presence of WDR62 protein (Figure 5, C and D). This is consistent with the inability of WDR62 to associate with either ERK or p38 MAPKs (Figure 4B).

WDR62-dependent JNK Activation Fails to Potentiate AP-1 Transcription

The consequence of JNK activation typically results in c-Jun phosphorylation leading to an increased transcription of AP-1–dependent genes. To examine whether or not WDR62 mediates this form of JNK activation toward AP-1 transcription, we measured AP-1–dependent transcription by using a luciferase reporter plasmid placed under the control of four tandem repeats of SV40 AP-1–binding elements (4 X AP-1-luciferase). HEK-293T cells were cotransfected with AP-1 reporter plasmid either alone or in the presence of WDR62 expression plasmid. Luciferase activity was measured 24 h after transfection in the absence of external stimuli (Figure 5E). Although AP-1 reporter alone resulted in a basal luciferase activity, coexpression with WDR62 resulted in a significant threefold reduced AP-1–dependent luciferase activity ($p < 0.05$, Figure 5E). To examine the AP-1–dependent transcription regulation by WDR62 in the presence of a persistent signal, we used expression plasmids encoding either MEKK activated form (ΔMEKK) or a JNKK2-JNK1 chimera. Both proteins have previously been shown to potentiate AP-1–dependent transcription through the JNK-c-Jun classical pathway (Zheng *et al.*, 1999; Holmberg *et al.*, 2002). Indeed, cotransfection of either ΔMEKK or JNKK2-JNK1 chimera resulted in 4- and 3.6-fold increase in AP-1 luciferase activity respectively (Figure 5E). However, the increase in AP-1 activity was completely abrogated in the presence of Myc-WDR62 ($p < 0.05$). Thus, although WDR62 is able to activate JNK kinase activity, JNK activation does not result in the classical signaling pathway leading to c-Jun phosphorylation and the corresponding increase in AP-1–dependent transcription.

WDR62 Localization Immunofluorescence

A possible explanation for the inability of WDR62 to result in c-Jun/AP-1 transcription activation could be that WDR62 is localized to a nonnuclear compartment. Indeed, WDR62 overexpression in HEK-293T cells resulted in granular cytoplasmic staining (Figure 2A). To identify the WDR62 containing granules, we used fluorescently labeled protein markers. These included cotransfection of WDR62 together with the following markers: early endosomes (EEA1-GFP), endoplasmic reticulum (M1-CFP), and golgi (GALT-CFP). None of the fluorescently labeled markers colocalized with Myc-WDR62 protein (Supplemental Figure S4). Therefore, we next stained HEK-293T cells for endogenous WDR62. HEK-293T cells exhibited dispersed faint cytoplasmic staining (see, for example, the nontransfected cells in Figure 7). We hypothesized that the granular cytoplasmic staining observed with anti-WDR62 antibodies is localized in cellular aggregates known as SGs. To examine this hypothesis, we transfected HEK-293T cells with fluorescently labeled proteins, known to form SGs upon overexpression. HEK-293T cells were transfected with either the T-cell intracellular antigen (YFP-TIA) or Tristetraprolin (YFP-TTP). Fixed cells were costained with anti-WDR62 (3G8) and analyzed using confocal microscopy (Figure 6A). Both YFP-TIA and YFP-TTP transfected cells display large granules. Interestingly, endogenous WDR62 displayed colocalization with both YFP-TIA and YFP-TTP into the SGs (Figure 6A). In contrast, GFP-G3BP, which is also known to forms large SGs upon overexpression in HEK-293T cells, failed to localize endogenous WDR62 protein into these granules (Figure 6A). To examine whether or not the recruitment of WDR62 to SGs also correlates with colocalization and activation of JNK, HEK-293T transfected with YFP-TIA, YFP-TTP or GFP-G3BP was costained with anti-phospho-specific JNK antibodies (Figure 6B). Consistent with the localization obtained with anti-WDR62 antibodies, phospho-JNK antibodies displayed SG staining when YFP-TIA and YFP-TTP were overexpressed but not by GFP-G3BP (Figure 6B), demonstrating that similar signaling specificity recruits WDR62 and an activated form of JNK to SGs. In addition, the SGs formed by TTP/TIA overexpression are distinct from those formed by G3BP (see below).

We next examined whether or not WDR62 is recruited to SGs after stimuli that are known to result in phosphorylation of translation initiation factor 2 α leading to translation arrest and generation of SGs containing stalled mRNA. Toward this end, HEK-293T cells were either untreated or treated with puromycin, arsenite, or arsenite + puromycin and heat shock (Figure 7). Cells were fixed and costained with a stress granule marker (anti-TIA, green), PB marker (anti-DCP1α, red), and WDR62 (anti-WDR62, 3G8, purple). Cell nuclei were stained with DAPI (blue). Puromycin treatment resulted in an increase in the number of PBs, whereas

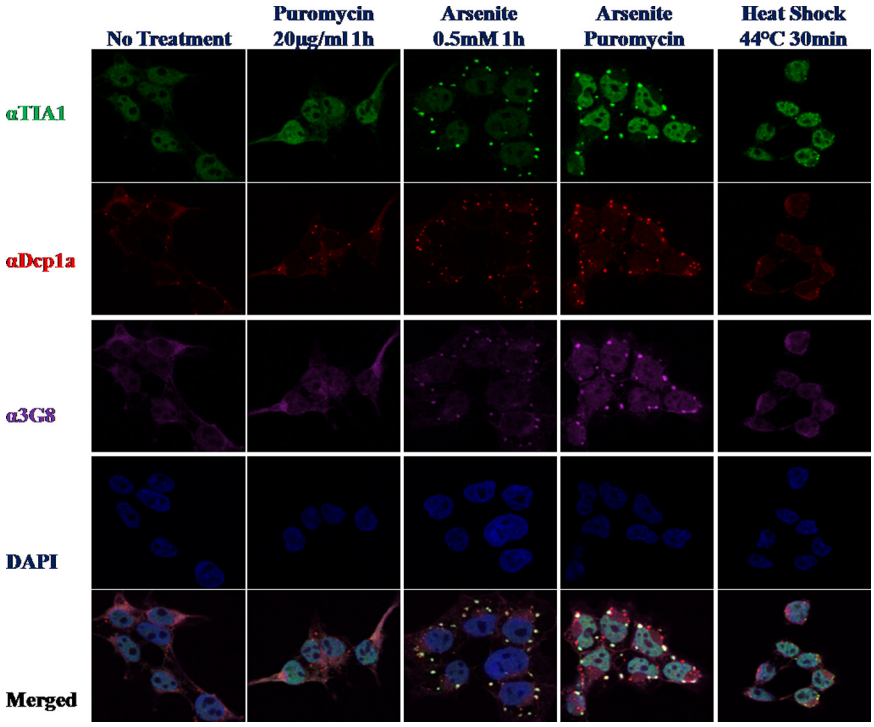

Figure 7. WDR62 is recruited to SG after different cellular stresses. Immunofluorescence of untreated HEK-293T cells or treated as indicated. Fixed cells were immunostained for SG marker (αTIA, green), PB marker (αDCP1α, red), WDR62 (α3G8, purple), and DAPI nuclear stain (blue). Representative images from confocal microscope are shown.

TIA staining remains in the nucleus and WDR62 is dispersed in the cytoplasm. Arsenite treatment resulted in the appearance of numerous SGs and PBs as observed by the increase staining for TIA and DCP1α markers. In addition, WDR62 staining displays colocalization with TIA but not DCP1α. Costimulation of arsenite with puromycin results in a reduced number of SGs but a significant increase in their size. This is observed for both TIA and WDR62 staining. On the other hand, PBs displayed only an increase in size (Figure 7). The merge panel clearly demonstrates that WDR62 is colocalized to SGs, but no colocalization is observed in PBs. Statistical analysis of stained cells revealed that the weighted costaining coefficient for WDR62-TIA and phospho-JNK-DCP1α colocalization is between 0.9-1 (Supplemental Figure S5). Cells exposure to 44°C for 30 min resulted in the generation of few SGs and PBs, which consistently exhibits costaining of TIA with WDR62 but not with DCP1α. To identify the localization of active JNK following the abovementioned stimuli, we used anti-phospho JNK antibody along with TIA and WDR62 antibodies (Figure 8). Although no staining for phospho-JNK is observed with puromycin treatment alone, arsenite and arsenite + puromycin treatments resulted in a strong nuclear staining as well as granular cytoplasmic staining that did not colocalize with either TIA or WDR62 (Figure 8). In contrast, the granular phospho-JNK staining colocalized with DCP1α in PB (see Figure 11B). Furthermore, after heat shock, phospho-JNK displays mainly strong nuclear localization. Merge images clearly demonstrate a distinct staining for phospho-JNK with either TIA or WDR62. Collectively, both artificial formation of SG by overexpression of SG-resident proteins and stimuli that result in SG formation lead to the recruitment of WDR62 to SGs and activated JNK to either SGs or PBs, respectively (Figures 7 and 8).

The fact that overexpression of GFP-G3BP resulted in the formation of SGs, yet, failed to recruit WDR62 and phospho-JNK to the artificially generated SGs, suggests that the granules formed are distinct. To examine whether endogenous G3BP protein is recruited to SGs, we stained cells with anti-G3BP after arsenite treatment and confirmed the colocalization of G3BP with the SG marker TIA (Supplemental Figure S6), consistent with previous reports (Kedersha *et al.*, 2005; Kedersha and Anderson, 2007). Thus, the protein content of the granules formed by G3BP overexpression is distinct from those formed by arsenite.

WDR62 Expression Level after Stress

We sought to follow WDR62 expression after stimuli that induce the formation of SGs. We subjected cell lysate derived from HEK-293T cells treated with arsenite to SDS-PAGE and Western blot with anti-WDR62 antibody. The WDR62 expression level is elevated after arsenite treatment (Figure 9A). In addition, UV irradiation resulted in an increase in WDR62 as well. The increase in WDR62 expression parallels the increase in JNK activity as observed by anti-phospho-JNK (Figure 9A). To examine whether the increase in WDR62 expression level is due to an alteration in its mRNA level, we used RT-PCR of cDNA derived from mRNA of HEK-293T cells treated with arsenite. WDR62 mRNA level remained unchanged after arsenite treatment (Figure 9B). Therefore, the increase in WDR62 protein expression after arsenite treatment is due to either an increase in WDR62 translation or protein stability. To examine whether or not JNK activity is required for the arsenite-dependent elevation in WDR62 expression, we used the specific JNK inhibitor SP600125 and followed WDR62 expression in the presence and absence of arsenite. Interestingly, the use of the JNK inhibitor suppressed the basal WDR62 expression level and the induced WDR62 expression after arsenite stimulation (Figure 9C). As expected, the JNK inhibitor SP600125 also resulted in down-regulation of c-Jun expression and c-Jun phosphorylation (Figure 9C, middle panels). Thus, JNK kinase activity per se is responsible for the increase in WDR62 expression level after arsenite treatment. WDR62 harbors multiple serine and threonine residues followed by a proline residue which is a typical

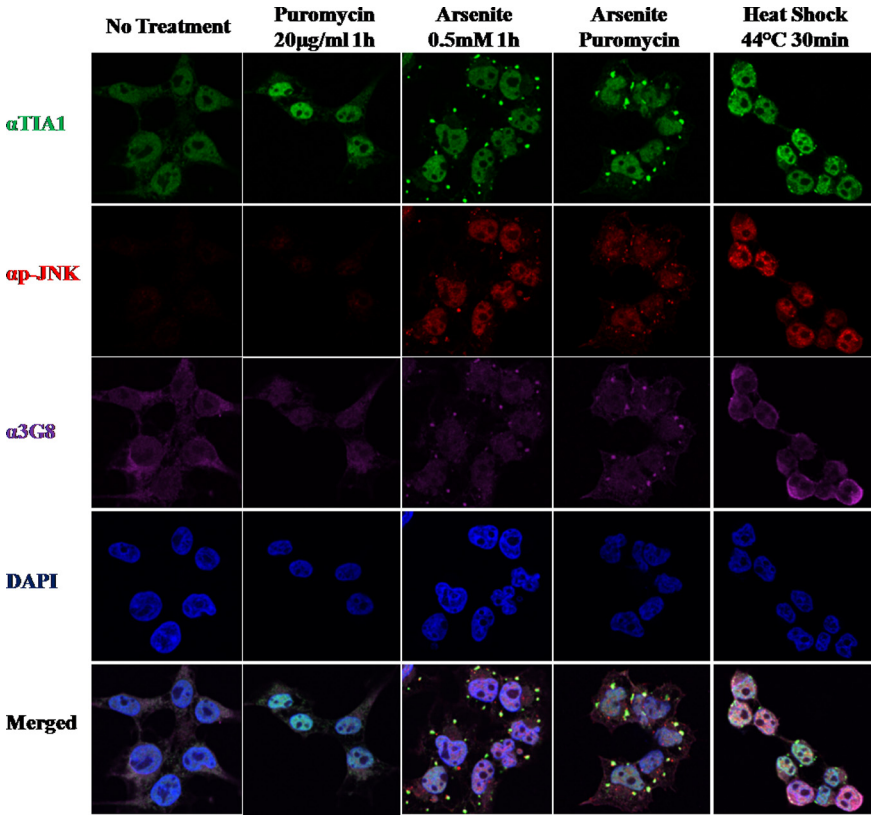

Figure 8. Activated-JNK is recruited to PB after different cellular stresses. Immunofluorescence of untreated HEK-293T cells or treated as indicated. Fixed cells were immunostained for SG marker (αTIA, green), activated-JNK (αp-JNK, red), WDR62 (α3G8, purple), and DAPI nuclear stain (blue). Representative images from confocal microscope are shown.

MAPK phospho-acceptor site. We used bacterially purified GST-fusion proteins to examine whether or not some of these potential MAPK phospho-acceptor sites can serve as JNK substrates in vitro. Indeed, GST-JBP5 and WDR62-C fragments encoding the C-terminal 505 and 309 amino acids, respectively, were efficiently phosphorylated by JNK (Supplemental Figure S7, lanes 3 and 4). WDR62 C-terminal domain contains several potential SP sites. GST-JBP5 purified fragment lacking the last six potential JNK phosphorylation sites completely lost its ability to be phosphorylated by JNK (Supplemental Figure S7, lanes 5 and 6). This suggests that WDR62 can serve as JNK substrate and phosphorylation is mapped to the six potential serine residues followed by proline located at the C-terminus.

We next examined whether JNK activation and subsequently WDR62 phosphorylation affect the association between WDR62 and JNK. We first used arsenite as a transient signal to activate JNK and tested WDR62-JNK interaction by coimmunoprecipitation. HEK-293T cells were cotransfected with HA-JNK2 and Myc-JBP5 encoding plasmids. Twenty-four hours after transfection cells were either untreated or treated with arsenite for 30 min. Coimmunoprecipitation was performed with anti-Myc and precipitated proteins were subjected to SDS-PAGE, Western blotting, and probed sequentially with anti-HA and anti-Myc antibodies. As expected, HA-JNK2 was efficiently precipitated only in cell lysate that expressed Myc-JBP5 protein (Figure 10A, left panel, lanes 3 and 7) and not in control lysate either lacking Myc-JBP5 or HA-JNK2 (Figure 10A, left panel, lanes 1, 2, 4, 5, 6, and 8). Moreover, HA-JNK2 coprecipitation was as efficient independent of the arsenite treatment.

We next examined the effect of WDR62 overexpression on phospho-JNK localization after arsenite treatment. HEK-293T cells were transfected with plasmid encoding Myc-WDR62 and stained for anti-phospho-JNK in the presence or absence of arsenite. In the absence of arsenite phospho-JNK staining is very low and mostly cytoplasmic. After arsenite treatment most of phospho-JNK staining is localized to the nucleus and PB. However, WDR62 overexpressing cells (white arrow) displayed a reduced nuclear phospho-JNK staining (Supplemental Figure S8).

To examine whether a persistent activation state of JNK may affect WDR62-JNK association, we used cotransfection of Myc-JBP5 encoding plasmid either alone or with one of the three after JNK1 expression plasmids encoding HA-JNKK2-JNK1 (JNK is activated persistently by its upstream MAP2K), HA-JNK1 APF (JNK1 mutant in its TGY-dual phosphorylation site and thus cannot be activated by the upstream kinase MKK4/7), and HA-JNK1 (wild type JNK1). Cells were harvested 24 h after transfection, and lysate was used in immunoprecipitation with anti-HA antibody. Purified proteins were subjected to SDS-PAGE and Western blotting and probed sequentially with anti-HA and anti-Myc antibodies. Myc-JBP5 was efficiently precipitated from cell lysate that coexpressed HA-JNK protein independent of the activation state of JNK (Figure 10B, left panel, lanes 5-7). Control lysates lacking either HA-JNK protein or Myc-JBP5 failed to produce a signal with anti-Myc antibody. Collectively, we suggest that both JNK activation state and WDR62 phosphorylation at the carboxy terminal do not affect WDR62-JNK association. Further studies are currently being conducted to reveal the functional role of the WDR62 JNK phosphorylation.

To examine whether or not JNK activity plays a role in SG formation or dynamic, we treated HEK-293T cells with the JNK inhibitor (SP600125) in the presence and absence of arsenite. Subsequently, cells were fixed and stained for SGs (TIA) and PBs (DCP1α). JNK inhibition after arsenite treat-

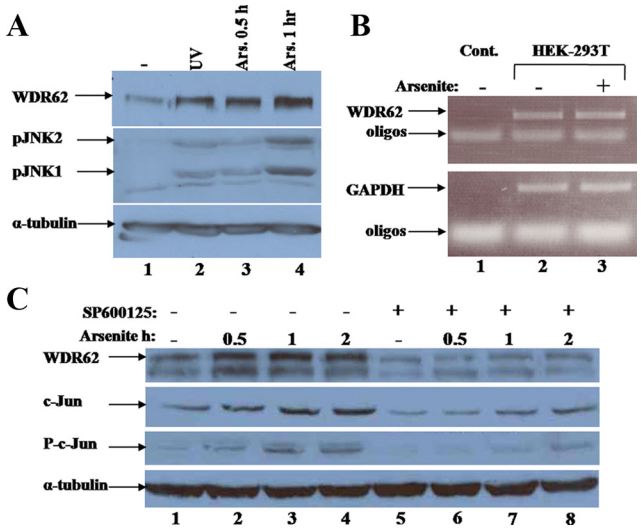

Figure 9. WDR62 expression is posttranscriptionally regulated by JNK. (A) Western blot analysis with cell lysate derived from HEK-293T cells treated as indicated. The expression levels of WDR62 (top panel), phospho-JNK (middle panel), and α-tubulin (lower panel) are shown. (B) RT-PCR with cDNA derived from HEK-293T cells treated as indicated. PCR was performed with WDR62- (top panel) and GAPDH- (bottom panel) specific oligonucleotides. (C) Western blot analysis with HEK-293T cells treated with arsenite as indicated in the absence or presence of JNK inhibitor, SP600125. The expression level of: WDR62 (top panel), c-Jun (second top panel), phospho-Jun (second bottom panel), and α-tubulin (lower panel) with the corresponding antibodies is shown.

ment resulted in a significant increase in the number of SGs ($p < 0.05$) but the SG formed were smaller in size ($p < 0.01$) compared with the SGs formed in the absence of SP600125 (Figure 11A and Supplemental Figure S9). Furthermore, cells treated with arsenite in the presence of SP600125 displayed a significant increase in the number of PBs with a reduced size (Figure 11B and Supplemental Figure S9, $p < 0.05$). Collectively, we suggest that JNK activity plays a role in SG and PB formation and may regulate the mRNA fate in the cytoplasm after cell stress that involves phosphorylation of eIF2α.

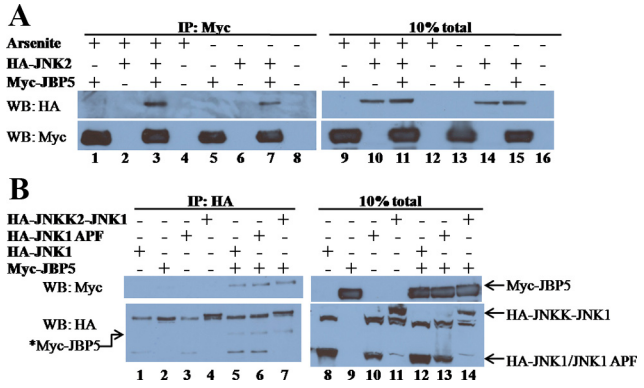

Figure 10. WDR62-JNK association is independent of transient and persistent activation signal. (A) HEK-293 cells were cotransfected as indicated. After 24 h, cells were either untreated or treated for 30 min with 0.5 mM arsenite. Cell lysate was coimmunoprecipitated with anti-Myc antibody and eluted proteins (left panel) as well as total cell lysate (right panel) were separated by SDS-PAGE, followed by Western blotting and probed with anti-HA (top panel) and anti-Myc (bottom panel) antibodies. (B) Cells were cotransfected as indicated. Cell lysate was coimmunoprecipitated with anti-HA antibody and eluted proteins as well as total cell lysate were treated as in A. The migration of the different HA-JNK proteins is indicated (right panel). *Myc-JBP5 migration is indicated (left panel) due to remaining signal from the αMyc antibody shown on the top panel.

DISCUSSION

The JNK signaling pathway plays a major role in diverse cellular functions. To do so, the JNK proteins require a protein network that allows an efficient activation platform to identify its specific substrate spatially and temporally. To isolate proteins associated with JNK, we designed a JNK bait protein composed of inactive JNK1 to screen the skeletal muscles and testes cDNA expression libraries using the RRS system. One of the clones, WDR62, is a previously uncharacterized protein that displays a specific binding to JNK. Interestingly, a high-throughput study using pairwise interaction with the yeast two-hybrid system revealed the association between WDR62 with JNK2 (Rual *et al.*, 2005). Here, using the RRS as an unbiased approach, we confirmed the interaction between JNK1 and WDR62 in yeast, and JNK1–2 and the upstream regulator MKK7 with WDR62 in tissue culture cells. WDR62 is ubiquitously expressed in all human tissues and cell lines tested, with increased expression in heart, skeletal muscles, and testes. Consistently, gene array data available from www.genecards.org confirmed the tissue panel expression pattern (Supplemental Figure S1B).

The JBP5-encoded protein fragment displays 27% sequence identity with JNKBP1, a previously characterized JNK scaffold protein that enhances JNK activation by MEK kinase and TAK1 (Koyano *et al.*, 1999). Interestingly, JNKBP1 contains four N-terminal WD40 domains, and WDR62 is composed of 12 WD40 domains. WD40 repeats (also known as WD or β-transducin repeats) are short ~40-amino acid motifs, often terminating in a Trp-Asp (W-D) dipeptide. WD-containing proteins are predicted to form a circulated beta-propeller structure. WD-repeat proteins are found in all eukaryotes and are implicated in a variety of functions ranging from signal transduction and transcription regulation to cell cycle control and apoptosis. The underlying common function of all WD-repeat proteins is coordinating multiprotein complex assemblies, in which the repeating units serve as a rigid scaffold for protein interactions (Garcia-Higuera *et al.*, 1996). The WD40 domain of WDR62 does not play a role in association/activation of JNK and MKK7, since JBP5 lacks the WD40 domains associated with both JNK and MKK7. In addition, because both JBP5 and full-length WDR62 when overexpressed are localized into granules, the WD40 domain plays no role in WDR62 cellular localization.

Here we demonstrated that endogenous WDR62 and JNK are recruited to SGs upon cotransfection with YFP-TTP and YFP-TIA but not with GFP-G3BP. Overexpression of many stress granule-associated proteins is known to induce spontaneous SGs in the absence of additional stress (Kedersha *et al.*, 2005). Although TIA possesses a prion-like aggregation activity (Gilks *et al.*, 2004) and TTP requires protein kinase R activity (PKR) to result in SG assembly, both TIA and TTP are RNA-binding proteins. G3BP, on the other hand, demonstrates an oligomerization domain that is regulated by phosphorylation (Tourriere *et al.*, 2003). These differences may lay their differential ability to recruit WDR62 and phospho-JNK to SGs.

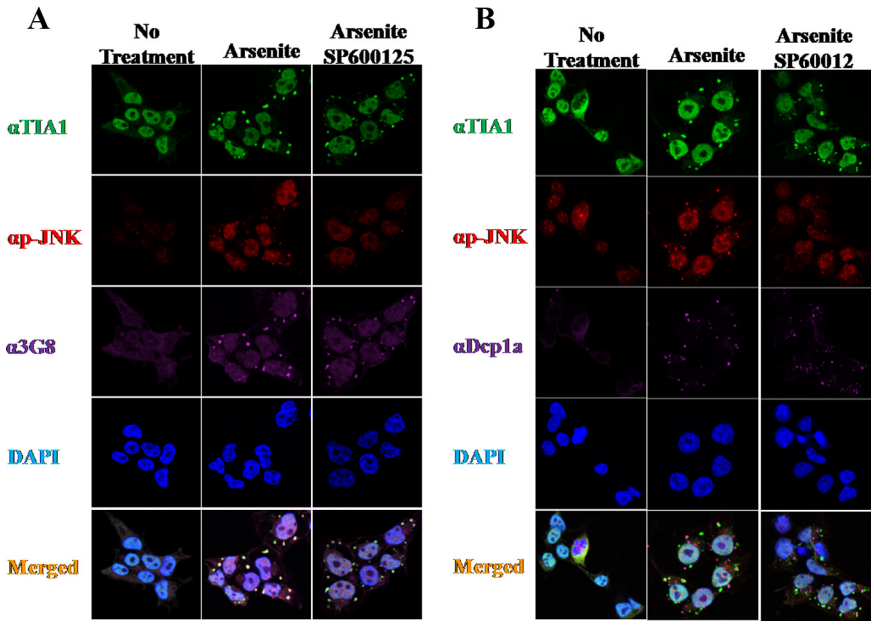

Figure 11. JNK inhibition affects the efficiency of SG and PB formation. Immunofluorescence of HEK-293T cells treated as indicated. Fixed cells were coimmunostained for (A) SG marker (αTIA, green), activated-JNK (αp-JNK, red), WDR62 (α3G8, purple), and DAPI nuclear stain (blue). (B) SG marker (αTIA, green), activated-JNK (αp-JNK, red), PB marker (αDCP1α, purple), and DAPI nuclear stain (blue). Representative images from confocal microscope are shown.

Exposure of cells to arsenite leads to the phosphorylation of the translation factor eIF2α, leading to polysome disassembly and SG and PB formation. Cellular staining of arsenite treated cells for WDR62 and phospho-JNK proteins reveals distinct staining to SGs and PBs, respectively. Whether or not the arsenite-activated form of JNK is localized initially to SGs and thereafter is translocated to PBs awaits further examination. Although JBP5 preserves the association with both activated JNK and after arsenite treatment (Figure 10), the binding of the full-length WDR62 to the endogenous activated JNK is yet to be examined. Nevertheless, it is demonstrated that JNK activity is important for SG assembly and formation of fully developed PBs. Taking into consideration that JNK activity is not completely inhibited by SP600125, the role of JNK in the SG assembly may be underestimated. In addition, JNK activity is crucial for phosphorylation and stabilization of WDR62 protein. WDR62 contains multiple S/TP potential MAPK phosphorylation sites. Using in vitro kinase assay, we were able to map six potential JNK phosphorylation sites located at the C-terminal domain (Supplemental Figure S7). Further research is required to map the JNK phosphorylation sites within WDR62 and examine their role in WDR62 stability and localization to SGs.

So far no one has been able to purify isolated SGs and PBs; nevertheless, the granules are morphologically defined by using immunostaining. Stress granules are composed mainly of mRNA, mRNA binding proteins with a known function in translational control, mRNA stability and metabolism, preinitiation and translation-related factors and signaling proteins with no known direct link to RNA metabolism. Interestingly, only very few kinases were described to be recruited to SGs and PBs. Fas-activated serine-threonine

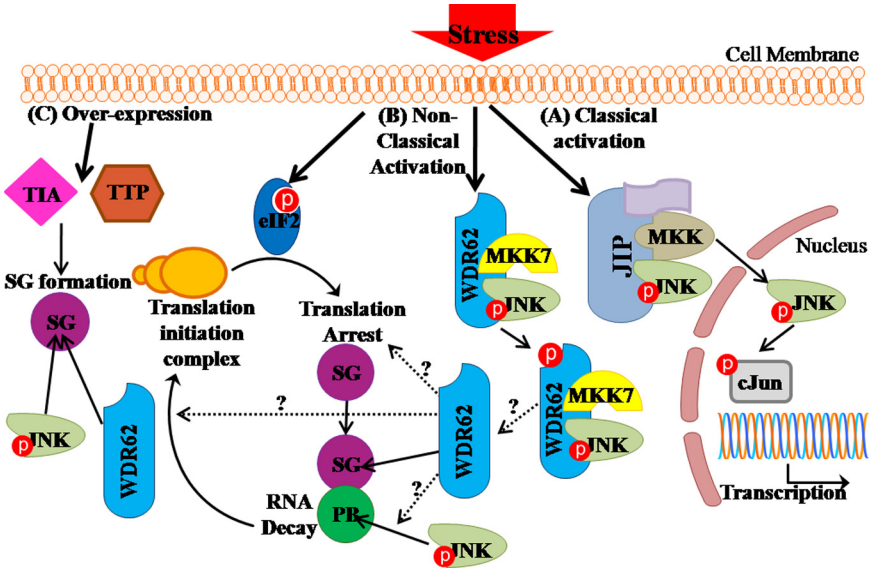

Figure 12. Schematic diagram summarizing JNK activation in response to cellular stress. (A) Classical JNK activation. (B) Nonclassical JNK activation by arsenite. (C) Artificial SG formation by either TTP or TIA overexpression. Dotted arrows with question marks are open questions remaining to be studied. Red circles represent phosphorylation.

phosphoprotein (FASTK) is recruited to SGs via its direct interaction with TIA. TRAF-2, which is a TNF-α receptor adaptor protein, is localized to SGs. TRAF-2 recruitment to SGs correlates with its inactivation upon stress. A recent study (Arimoto *et al.*, 2008) identified the scaffold protein, Receptor-activated protein kinase C (RACK1), which is localized to SGs after type 1 stresses (arsenite, heat-shock). RACK1 binds the stress responsive MAP 3K of the JNK pathway, MEKK4/MTK1. Interestingly, RACK1 is also composed of seven WD40 repeats. RACK1 recruitment to SGs results in reduced MTK1 activity in the cytoplasm, and it is suggested that this is part of the mechanism whereby cancer cells escape from apoptosis after chemotherapy (Arimoto *et al.*, 2008).

Stress granules are sites of mRNA triage at which a cellular decision is made to route the stalled mRNA to reinitiation, degradation, or storage. How these decisions are made is still an open question. However, protein kinases such as the JNK may play a role in determining the fate of mRNA. Therefore, identification of JNK substrates among the proteins involved in mRNA metabolism and stability is a crucial step in understanding the role of JNK in mRNA and cellular fate after cellular stress.

Previous studies highlighted the role of JNK in mRNA stability of VEGF (Pages *et al.*, 2000). In addition, JNK response elements were identified as being required for the stabilization of the IL-2 mRNA through the binding of nucleolin and YB1 (Chen *et al.*, 2000).

Although we made multiple efforts to reduce the endogenous WDR62 expression levels with siRNA technology, we failed to do so. A recently published study (Ohn *et al.*, 2008) aimed to screen for genes that are involved in the assembly of SGs and PBs using RNAi technology. This technology identified 101 human genes which are required for SG assembly. Both WDR62 and JNK were not identified in this screen, probably due to either failure to reduce their levels or gene redundancy.

Collectively, classical JNK activation after cellular stress results in JNK activation and its nuclear translocation (Figure 12A). This involves the association with scaffold proteins such as JIP and β-arrestin. Here, we have identified a novel JNK scaffold protein, WDR62. WDR62 is shown to associate with both JNK and MKK7. WDR62 takes part of a nonclassical activation of JNK in response to cellular stress (Figure 12B). WDR62 associates with JNK in resting cells as well as after either transient or persistent stress signal. WDR62 activates JNK and can serve as JNK substrate. Artificial formation of SGs by overexpression of either TIA or TTP recruits WDR62 and phospho-JNK to SGs (Figure 12C). Stress that leads to phosphorylation of translation initiation factor eIF2α results in translation arrest and the accumulation of stalled mRNA in SGs and PBs. After stress, JNK is activated and WDR62 expression level is increased due to posttranscriptional mechanism. Subsequently, WDR62 is recruited to SGs and phospho-JNK to PBs. We propose that WDR62 may connect JNK activation with mRNA homeostasis and cellular fate in response to stress.

ACKNOWLEDGMENTS

The authors thank Drs. Ofer Shenker and Edith Suss-Toby and Ms. Aviva Cohen for their excellent technical assistance and Professors Nancy Kedersha, Jamal Tazi, Mark Philips, Tuula Kallunki (Institute of Cancer Biology, Danish Cancer Society, Copenhagen, Denmark), and Michael Courtney for providing various fluorescently labeled proteins. Tal Hasin is supported by the Etai Sharon Z''l Rambam-Atidim Fellowship Fund for Academic Excellence. This work was supported by the Israeli Science Foundation Grant 641/07 to A.A.

REFERENCES

Arimoto, K., Fukuda, H., Imajoh-Ohmi, S., Saito, H., and Takekawa, M. (2008). Formation of stress granules inhibits apoptosis by suppressing stress-responsive MAPK pathways. Nat. Cell Biol. *10*, 1324–1332.

Aronheim, A., Broder, Y. C., Cohen, A., Fritsch, A., Belisle, B., and Abo, A. (1998). Chp, a homologue of the GTPase Cdc42, activates the JNK pathway and is implicated in reorganizing the actin cytoskeleton. Curr. Biol. *8*, 1125–1128.

Broder, Y. C., Katz, S., and Aronheim, A. (1998). The Ras recruitment system, a novel approach to the study of protein-protein interactions. Curr. Biol. *8*, 1121–1124.

Chang, L., and Karin, M. (2001). Mammalian MAP kinase signalling cascades. Nature *410*, 37–40.

Chen, C. Y., Gherzi, R., Andersen, J. S., Gaietta, G., Jurchott, K., Royer, H. D., Mann, M., and Karin, M. (2000). Nucleolin and YB-1 are required for JNK-mediated interleukin-2 mRNA stabilization during T-cell activation. Genes Dev. *14*, 1236–1248.

Dard, N., and Peter, M. (2006). Scaffold proteins in MAP kinase signaling: more than simple passive activating platforms. Bioessays *28*, 146–156.

Davis, R. J. (2000). Signal transduction by the JNK group of MAP kinases. Cell *103*, 239–252.

Garcia-Higuera, I., Fenoglio, J., Li, Y., Lewis, C., Panchenko, M. P., Reiner, O., Smith, T. F., and Neer, E. J. (1996). Folding of proteins with WD-repeats: comparison of six members of the WD-repeat superfamily to the G protein beta subunit. Biochemistry *35*, 13985–13994.

Gilks, N., Kedersha, N., Ayodele, M., Shen, L., Stoecklin, G., Dember, L. M., and Anderson, P. (2004). Stress granule assembly is mediated by prion-like aggregation of TIA-1. Mol. Biol. Cell *15*, 5383–5398.

Girardin, S. E., and Yaniv, M. (2001). A direct interaction between JNK1 and CrkII is critical for Rac1-induced JNK activation. EMBO J. *20*, 3437–3446.

Holmberg, C., Katz, S., Lerdrup, M., Herdegen, T., Jaattela, M., Aronheim, A., and Kallunki, T. (2002). A novel specific role for I kappa B kinase complex-associated protein in cytosolic stress signaling. J. Biol. Chem. *277*, 31918–31928.

Hubsman, M. Y., Aronheim, G., A. (2001). A novel approach for the identification of protein-protein interaction with integral membrane proteins. Nucleic Acids Res. *29*, e18.

Kadoya, T., Khurana, A., Tcherpakov, M., Bromberg, K. D., Didier, C., Broday, L., Asahara, T., Bhoumik, A., and Ronai, Z. (2005). JAMP, a Jun N-terminal kinase 1 (JNK1)-associated membrane protein, regulates duration of JNK activity. Mol. Cell. Biol. *25*, 8619–8630.

Katz, S., Heinrich, R., and Aronheim, A. (2001). The AP-1 repressor, JDP2, is a bona fide substrate for the c-Jun N- terminal kinase. FEBS Lett. *506*, 196–200.

Kedersha, N., and Anderson, P. (2007). Mammalian stress granules and processing bodies. Methods Enzymol. *431*, 61–81.

Kedersha, N. *et al.* (2005). Stress granules and processing bodies are dynamically linked sites of mRNP remodeling. J. Cell Biol. *169*, 871–884.

Kelkar, N., Gupta, S., Dickens, M., and Davis, R. J. (2000). Interaction of a mitogen-activated protein kinase signaling module with the neuronal protein JIP3. Mol. Cell Biol. *20*, 1030–1043.

Koyano, S., Ito, M., Takamatsu, N., Shiba, T., Yamamoto, K., and Yoshioka, K. (1999). A novel Jun N-terminal kinase (JNK)-binding protein that enhances the activation of JNK by MEK kinase 1 and TGF-beta-activated kinase 1. FEBS Lett. *457*, 385–388.

Marti, A., Luo, Z., Cunningham, C., Ohta, Y., Hartwig, J., Stossel, T. P., Kyriakis, J. M., and Avruch, J. (1997). Actin-binding protein-280 binds the stress-activated protein kinase (SAPK) activator SEK-1 and is required for tumor necrosis factor-alpha activation of SAPK in melanoma cells. J. Biol. Chem. *272*, 2620–2628.

Miller, W. E., and Lefkowitz, R. J. (2001). Expanding roles for beta-arrestins as scaffolds and adapters in GPCR signaling and trafficking. Curr. Opin. Cell Biol. *13*, 139–145.

Morrison, D. K., and Davis, R. J. (2003). Regulation of MAP kinase signaling modules by scaffold proteins in mammals. Annu. Rev. Cell Dev. Biol. *19*, 91–118.

Ohn, T., Kedersha, N., Hickman, T., Tisdale, S., and Anderson, P. (2008). A functional RNAi screen links O-GlcNAc modification of ribosomal proteins to stress granule and processing body assembly. Nat. Cell Biol. *10*, 1224–1231.

Pages, G., Berra, E., Milanini, J., Levy, A. P., and Pouyssegur, J. (2000). Stress-activated protein kinases (JNK and p38/HOG) are essential for vascular endothelial growth factor mRNA stability. J. Biol. Chem. *275*, 26484–26491.

Rual, J. F. *et al*. (2005). Towards a proteome-scale map of the human protein-protein interaction network. Nature *437*, 1173–1178.

Rubinfeld, H., and Seger, R. (2005). The ERK cascade: a prototype of MAPK signaling. Mol. Biotechnol. *31*, 151–174.

Shaul, Y. D., and Seger, R. (2007). The MEK/ERK cascade: from signaling specificity to diverse functions. Biochim. Biophys. Acta *1773*, 1213–1226.

Tibbles, L. A., and Woodgett, J. R. (1999). The stress-activated protein kinase pathways. Cell Mol. Life Sci. *55*, 1230–1254.

Tourriere, H., Chebli, K., Zekri, L., Courselaud, B., Blanchard, J. M., Bertrand, E., and Tazi, J. (2003). The RasGAP-associated endoribonuclease G3BP assembles stress granules. J. Cell Biol. *160*, 823–831.

Verhey, K. J., Meyer, D., Deehan, R., Blenis, J., Schnapp, B. J., Rapoport, T. A., and Margolis, B. (2001). Cargo of kinesin identified as JIP scaffolding proteins and associated signaling molecules. J. Cell Biol. *152*, 959–970.

Weston, C. R., Lambright, D. G., and Davis, R. J. (2002). MAP kinase signaling specificity. Science *296*, 2345–2347.

Xia, Y., Wu, Z., Su, B., Murray, B., and Karin, M. (1998). JNKK1 organizes a MAP kinase module through specific and sequential interactions with upstream and downstream components mediated by its amino-terminal extension. Genes Dev. *12*, 3369–3381.

Yasuda, J., Whitmarsh, A. J., Cavanagh, J., Sharma, M., and Davis, R. J. (1999). The JIP group of mitogen-activated protein kinase scaffold proteins. Mol. Cell. Biol. *19*, 7245–7254.

Zheng, C., Xiang, J., Hunter, T., and Lin, A. (1999). The JNKK2-JNK1 fusion protein acts as a constitutively active c-Jun kinase that stimulates c-Jun transcription activity. J. Biol. Chem. *274*, 28966–28971.

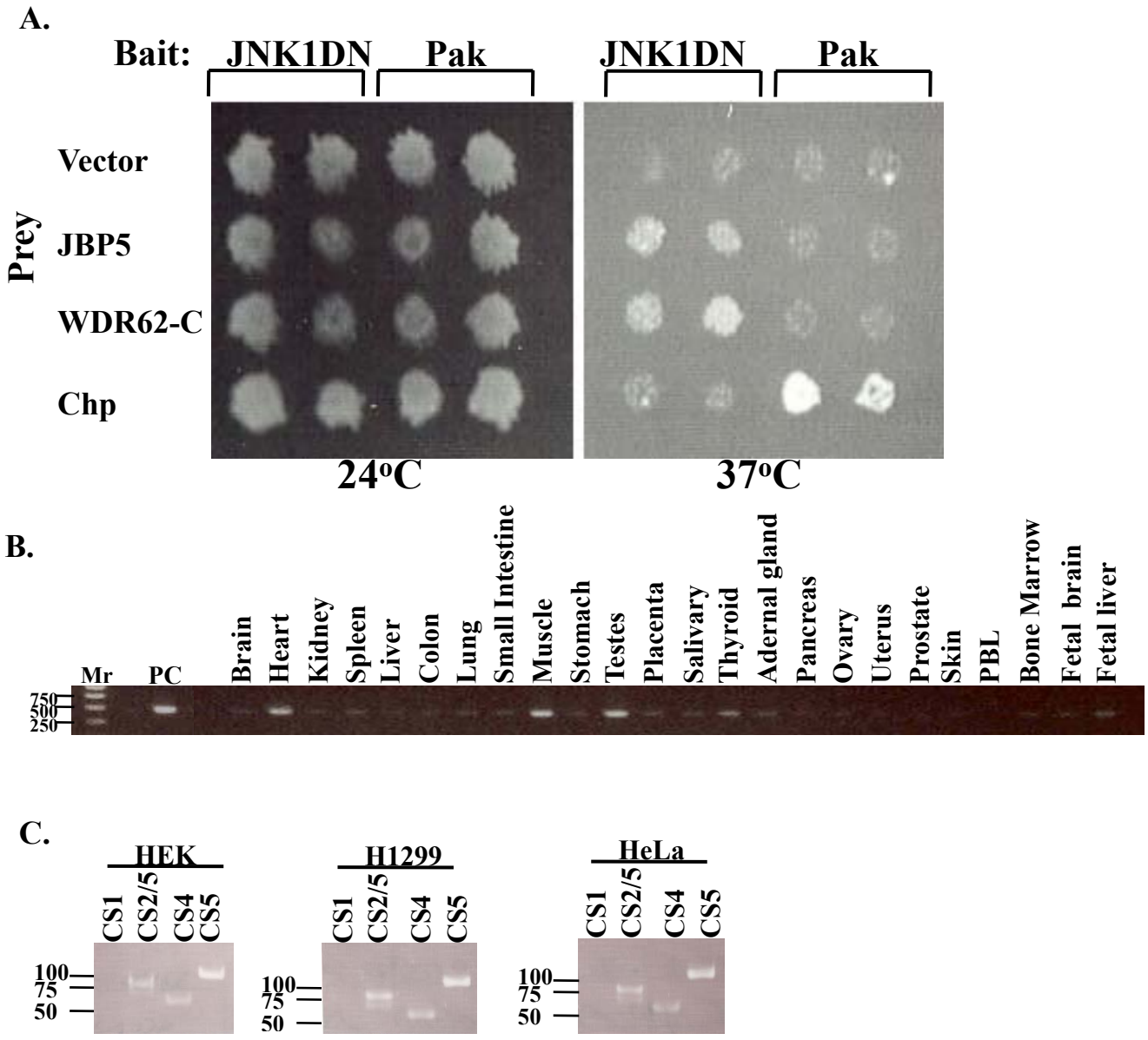

Sup-Figure 1 A-C

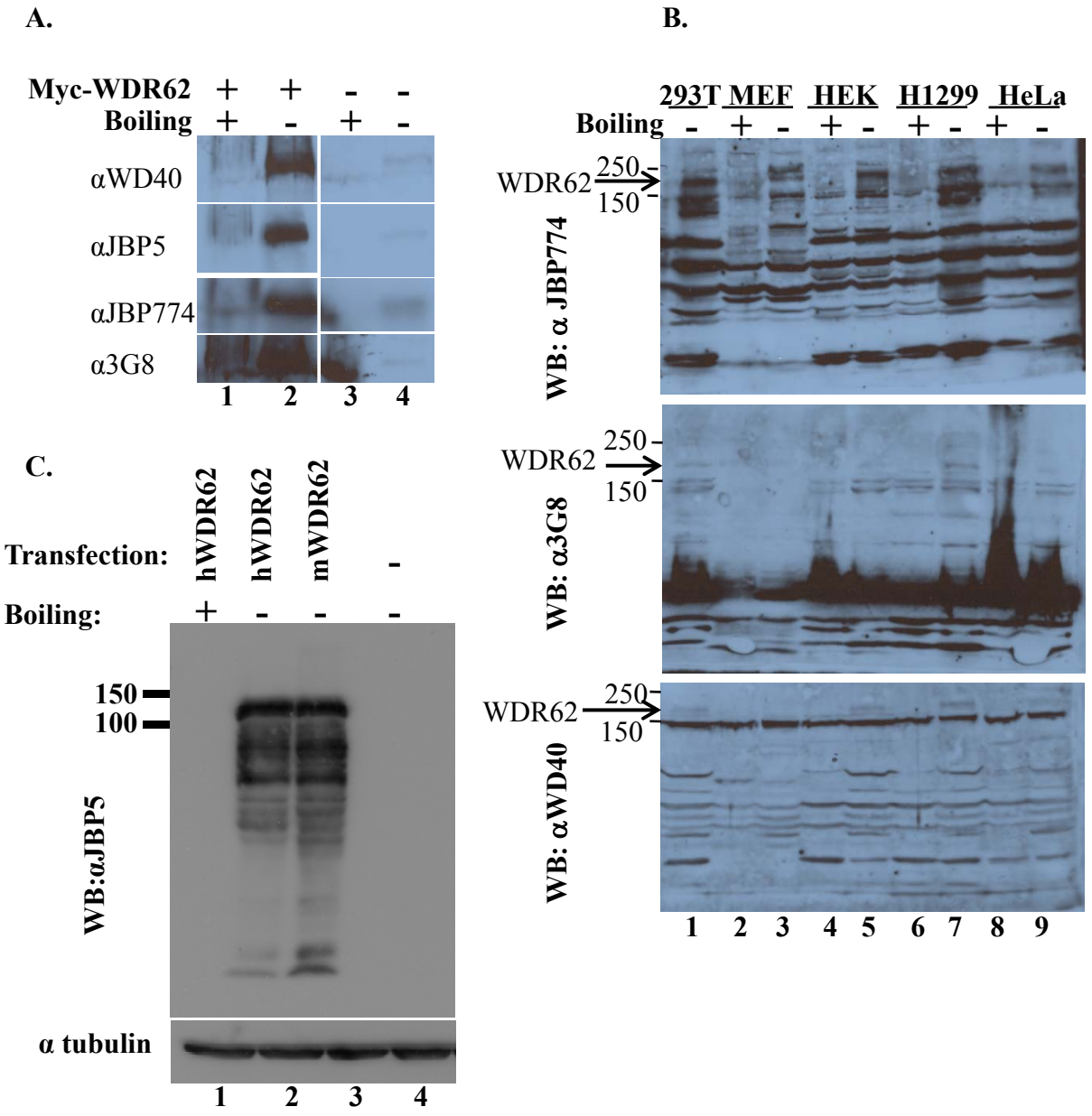

Sup-Figure 2 A-C

A.

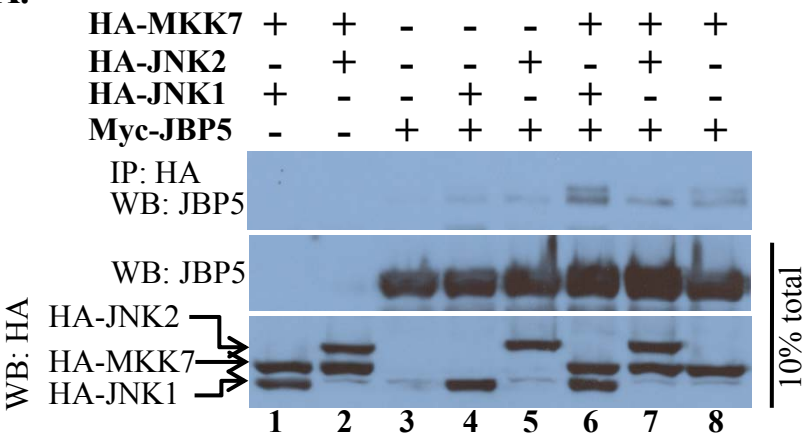

B.

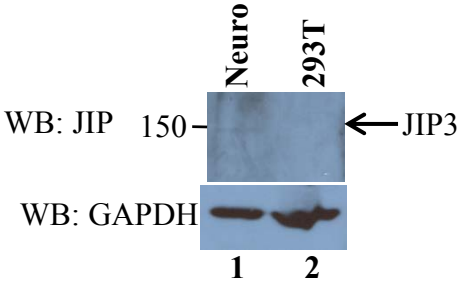

Sup-Figure 3

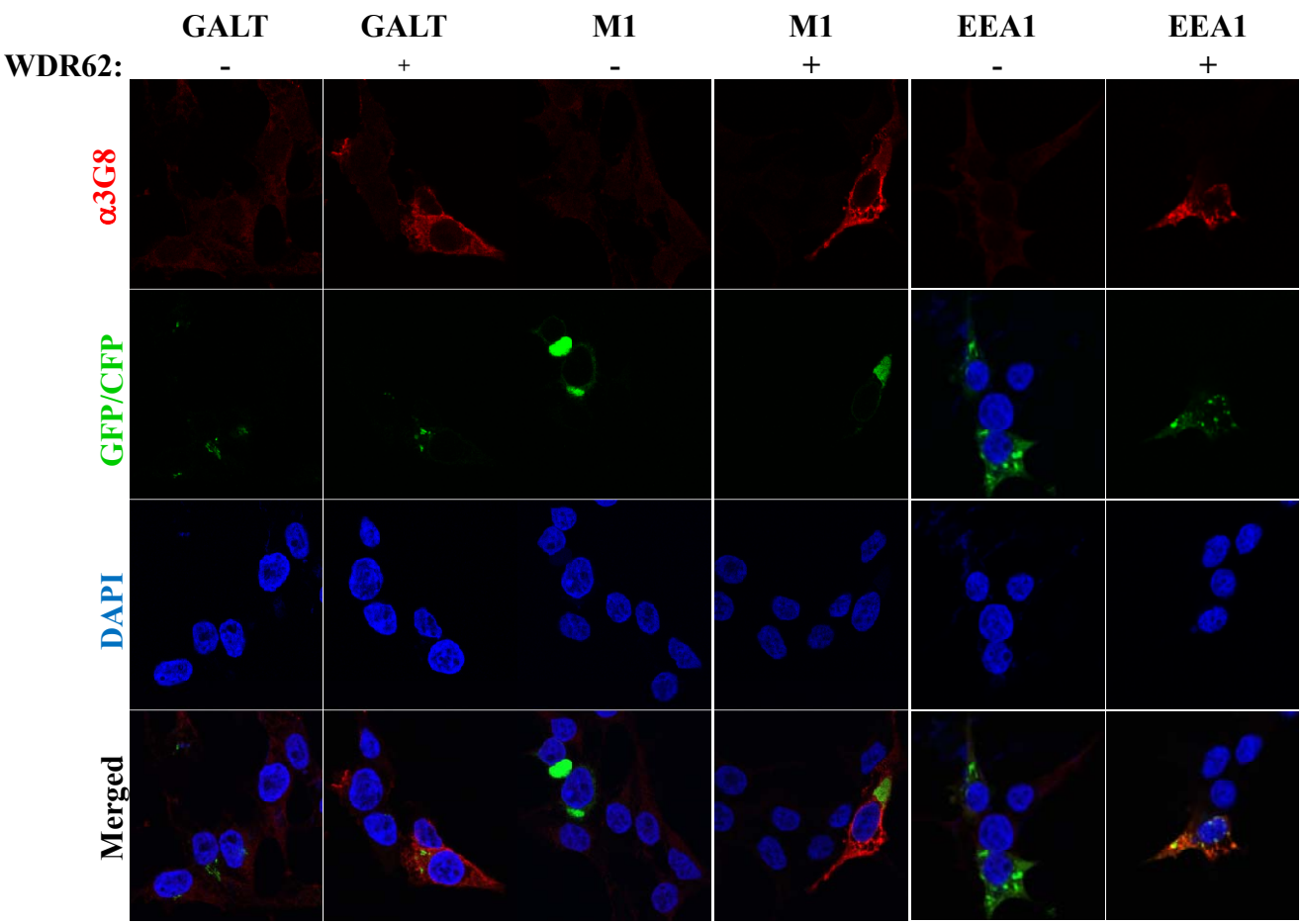

Sup-Figure 4

	Channel	Weighted Co -localization coefficient	n
WDR62 and TIA1 co-localization	WDR62	0.94±0.1	55
	TIA1	1±0.01	
phospho-JNK and DCP1α co-localization	pJNK	0.9±0.08	44
	DCP1a	0.94±0.07	

Sup-Figure 5

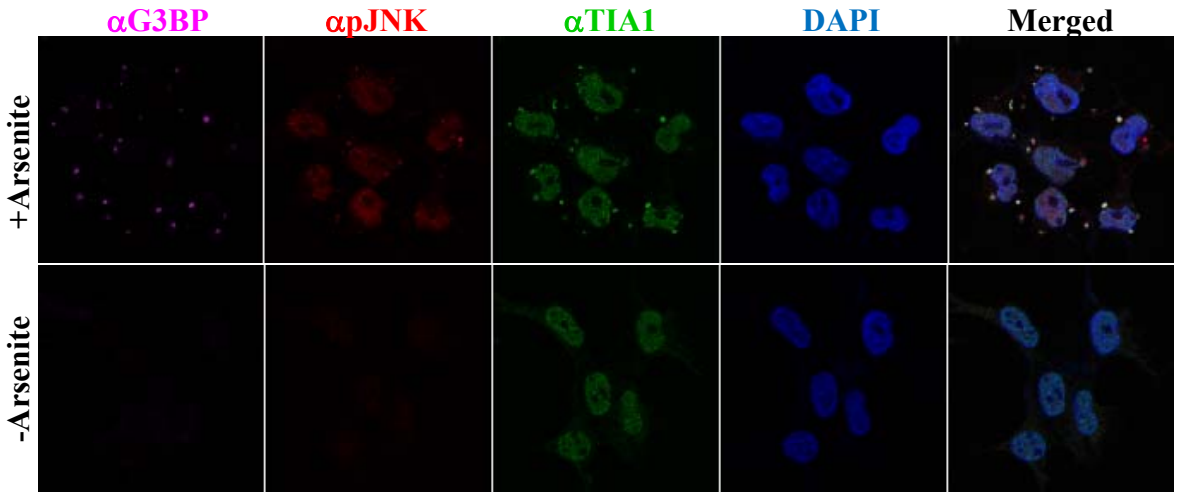

Sup-Figure 6

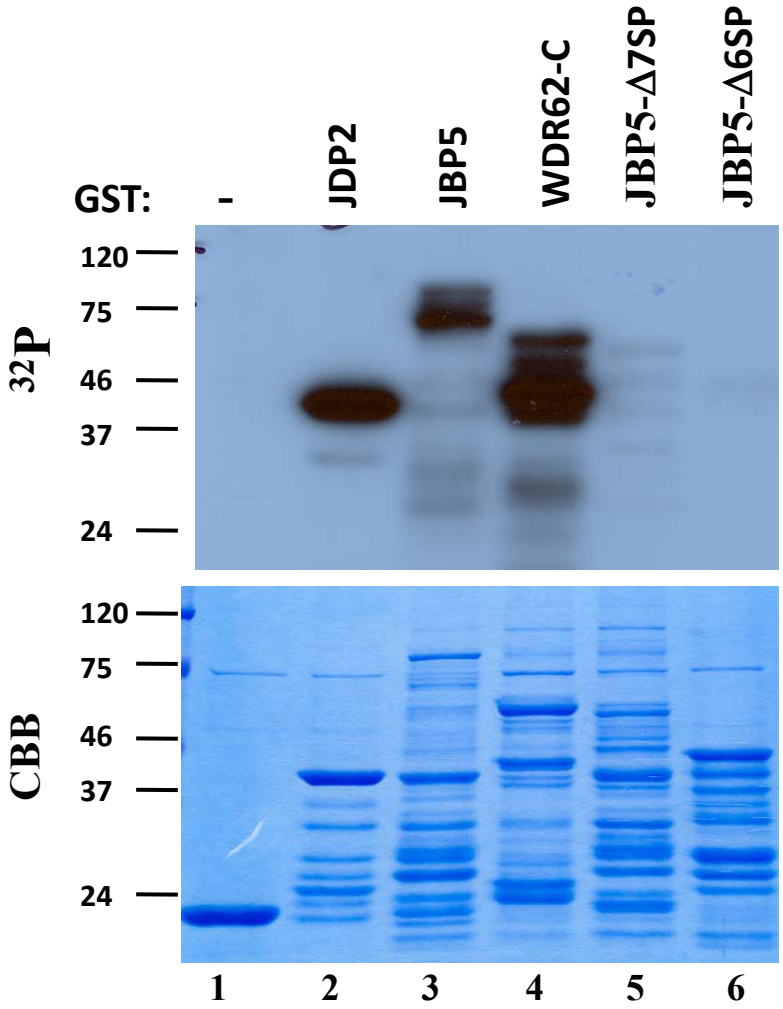
GST:
-
JDP2
JBP5
WDR62-C
JBP5-Δ7SP
JBP5-Δ6SP
32P
120
75
46
37
24
CBB
120
75
46
37
24
1
2
3
4
5
6

Sup-Figure 7

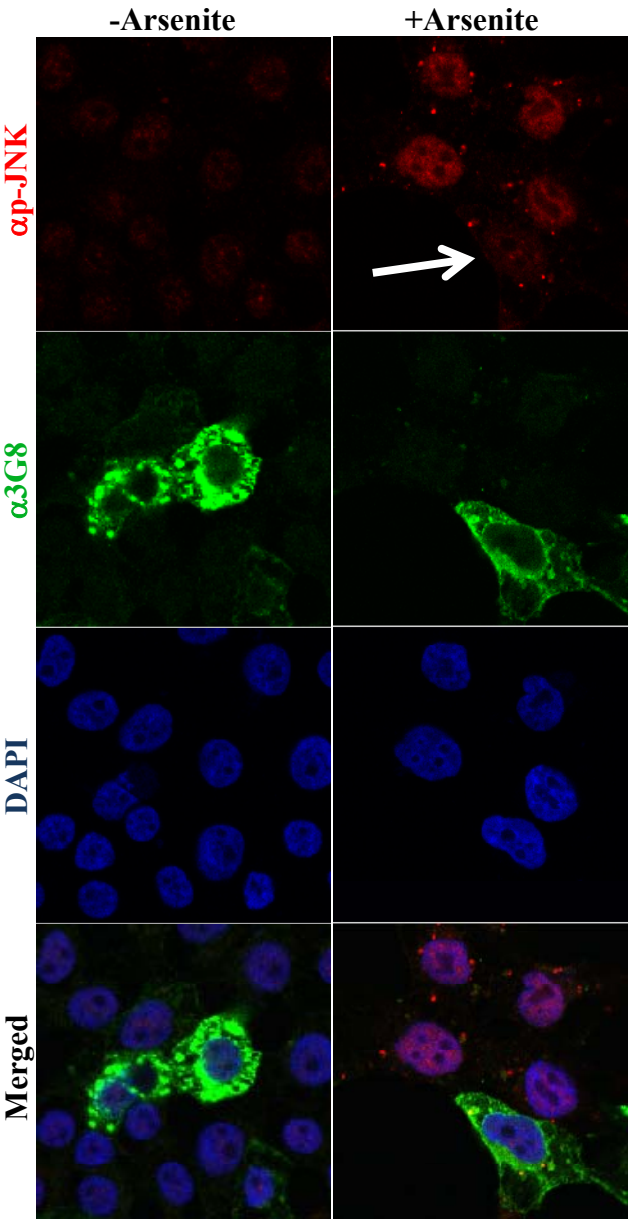

Sup-Figure 8

	Stress Granules			Processing Bodies		
Treatment	**No. per Cell**	**Average Size (pxl^2)**	**n**	**No. per Cell**	**Average Size (pxl^2)**	**n**
Arsenite	11.3±1.8*	58.6±7.7**	32	13.5±1.8*	26.2±5.3*	30
SP600125 Arsenite	13.6±1.4	42.5±5.2	25	15.1±2.0	20±2.0	31

Sup-Figure 9